and host protection against *Streptococcus pneumoniae* infection caused by pneumococcal polysaccharide vaccine, Oral presentation, Block Symposium, Immunology 2012 The American Society of Immunologists, Boston, May 4-8, 2012.

9. 金城雄樹, 朴 貞玉, 大石和徳, 川上和義. 肺炎球菌感染防御における NKT 細胞の役割の解析及び NKT 細胞の活性化を応用した肺炎球菌ワクチン開発. 第 5 回感染病態研究フロンティア. 8 月 4 日, 2012 年.

10. 宮坂智充, 青柳哲史, 内山美寧, 國島広之, 賀来満夫, 石井恵子, 中山俊憲, 植村靖史, 大石和徳, 金城雄樹, 宮﨑義継, 川上和義. 23 価肺炎球菌ワクチン接種後の抗体産生における NKT 細胞の役割に関する臨床免疫学的検討. 第 16 回日本ワクチン学会学術集会. 11 月 17-18 日, 2012 年, 横浜.

11. 宮坂智充, 外山真彦, 赤堀ゆきこ, 石井恵子, 金城雄樹, 宮﨑義継, 中山俊憲, 岩倉洋一郎, 西城 忍, 大石和徳, 川上和義. 23 価肺炎球菌多糖体ワクチンによる血清型特異的 IgG 産生における NKT 細胞と Dectin-2 の役割. 第 16 回日本ワクチン学会学術集会. 11 月 17-18 日, 2012 年, 横浜.

12. Miyasaka T, Akahori Y, Toyama M, Miyamura N, Ishii K, Saijo S, Iwakura Y, Kinjo Y, Kawakami K: Dectin-2-mediated sensing of pneumococcal polysaccharide vaccine leads to induction of serotype-specific IgG through NKT cells activation. Workshop, 第 41 回日本免疫学会学術集会, Kobe, December 5-7, 2012.

## H. 知的所有権の取得状況

1. 特許取得：なし
2. 実用新案登録：なし
3. その他：なし

# II. 研究成果に関する刊行一覧表

# 平成 22-24 年度厚生労働科学研究費補助金(創薬基盤推進研究事業)
# 研究成果に関する刊行一覧表

| 著者氏名 | 論文タイトル名 | 雑誌名 | 巻 | ページ | 出版年 |
|---|---|---|---|---|---|
| Kinjo Y, Illarionov PA, Vela JL, Pei B, Girardi E, Li X, Li Y, Imamura M, Kaneko Y, Okawara A, Miyazaki Y, Gomez-Velasco A, Rogers P, Dahesh S, Uchiyama S, Khurana A, Kawahara K, Yashilkaya H, Andrew PA, Wong CH, Kawakami K, Nizet V, Besra GS, Tsuji M, Zajonc DM, Kronenberg M | Invariant natural killer T cells recognize glycolipids from pathogenic Gram-positive bacteria | Nat Immunol | 12 | 966-974 | 2011 |
| Girardi E, Yu ED, Li Y, Tarumoto N, Pei B, Wang J, Illarionov P, Kinjo Y, Kronenberg M, Zajonc DM | Unique interplay between sugar and lipid in determining the antigenic potency of bacterial antigens for NKT Cells | PLoS Biol | 9 | e1001189 | 2011 |
| Kinjo Y and Ueno K | iNKT cells in microbial immunity: recognition of microbial glycolipids | Microbiol Immunol | 55 | 472-82 | 2011 |
| Miyasaka T, Aoyagi T, Uchiyama B, Oishi K, Nakayama T, Kinjo Y, Miyazaki Y, Kunishima H, Hirakata Y, Kaku M, Kawakami K | A possible relationship of natural killer T cells with humoral immune response to 23-valent pneumococcal polysaccharide vaccine in clinical settings | Vaccine | 30 | 3304-3310 | 2012 |

nature immunology

# Invariant natural killer T cells recognize glycolipids from pathogenic Gram-positive bacteria

Yuki Kinjo[1,2,13], Petr Illarionov[3,13], José Luis Vela[1,13], Bo Pei[1], Enrico Girardi[4], Xiangming Li[5], Yali Li[4], Masakazu Imamura[6], Yukihiro Kaneko[2], Akiko Okawara[2], Yoshitsugu Miyazaki[2], Anaximandro Gómez-Velasco[7], Paul Rogers[8], Samira Dahesh[9], Satoshi Uchiyama[9], Archana Khurana[1], Kazuyoshi Kawahara[10], Hasan Yesilkaya[11], Peter W Andrew[11], Chi-Huey Wong[6], Kazuyoshi Kawakami[12], Victor Nizet[9], Gurdyal S Besra[3], Moriya Tsuji[5], Dirk M Zajonc[4] & Mitchell Kronenberg[1]

**Natural killer T cells (NKT cells) recognize glycolipid antigens presented by CD1d. These cells express an evolutionarily conserved, invariant T cell antigen receptor (TCR), but the forces that drive TCR conservation have remained uncertain. Here we show that NKT cells recognized diacylglycerol-containing glycolipids from *Streptococcus pneumoniae*, the leading cause of community-acquired pneumonia, and group B *Streptococcus*, which causes neonatal sepsis and meningitis. Furthermore, CD1d-dependent responses by NKT cells were required for activation and host protection. The glycolipid response was dependent on vaccenic acid, which is present in low concentrations in mammalian cells. Our results show how microbial lipids position the sugar for recognition by the invariant TCR and, most notably, extend the range of microbes recognized by this conserved TCR to several clinically important bacteria.**



Natural killer T cells (NKT cells) fascinate immunologists because they have several unique features[1–5]. For example, NKT cells are responsive to glycolipids presented by CD1d, a nonpolymorphic major histocompatibility complex class I–like antigen-presenting molecule, in contrast to conventional T cells, which recognize peptide antigens. Furthermore, instead of the diverse antigen receptors expressed by most T cell populations, most NKT cells express an invariant T cell antigen receptor (TCR) α-chain formed by α-chain variable region 14–α-chain joining region 18 ($V_\alpha$14-$J_\alpha$18) rearrangement in mice and $V_\alpha$24-$J_\alpha$18 rearrangement in humans. Therefore, mouse NKT cells that express an invariant $V_\alpha$14 TCR are called '$V_\alpha$14*i* NKT cells' and their human counterparts are called '$V_\alpha$24*i* NKT cells' and this population is collectively called '*i*NKT cells'. Additionally, rodent and primate *i*NKT cells recognize the same antigens, and there is interspecies cross-reactivity[6]. This unusual degree of conservation of antigen recognition suggests that this specificity has a particularly important function.

Many reports have shown that *i*NKT cells participate in the response to microbial pathogens[1,2,5,7]. In some such cases, *i*NKT cells were probably responding not to a microbial glycolipid but instead were probably activated by inflammatory cytokines acting alone[8] and/or with self antigens presented by CD1d[2,7,9]. In contrast, two types of bacteria, *Sphingomonas* species[10,11] and *Borrelia burgdorferi*[12], have been shown to have glycolipid antigens for the *i*NKT cell TCR. *Helicobacter pylori* is also reported to have such antigens[13], although we have not confirmed reactivity with synthetic or purified material (J.L.V., A.K. and M.K., data not shown). Despite that discrepancy, none of these microbes cause lethal diseases and therefore it is unlikely that they are major drivers for the conservation of the *i*NKT cell TCR specificity throughout much of mammalian evolution.

Because of the conservation noted above, we reasoned that the *i*NKT cell TCR would recognize antigens of certain highly pathogenic bacteria. Worldwide, the most lethal bacterial pathogen is *Streptococcus pneumoniae*, an agent of pneumonia, bloodstream infection and meningitis in children and the elderly, now estimated to cause 11% of all deaths in children from 1 month to 5 years of age[14]. Notably, $V_\alpha$14*i* NKT cell–deficient $J_\alpha$18-deficient mice challenged with *S. pneumoniae* have considerable impairment in bacterial clearance from the lung and much lower survival[15]. The mechanism is related in part to interferon-γ (IFN-γ) derived from $V_\alpha$14*i* NKT cells, which facilitates bacterial clearance by stimulating tumor necrosis

[1]Division of Developmental Immunology, La Jolla Institute for Allergy & Immunology, La Jolla, California, USA. [2]Department of Chemotherapy and Mycoses, National Institute of Infectious Diseases, Tokyo, Japan. [3]School of Biosciences, University of Birmingham, Edgbaston, Birmingham, UK. [4]Division of Cell Biology, La Jolla Institute for Allergy & Immunology, La Jolla, California, USA. [5]HIV and Malaria Vaccine Program, Aaron Diamond AIDS Research Center, Affiliate of the Rockefeller University, New York, New York, USA. [6]Department of Chemistry and Skaggs Institute for Chemical Biology, The Scripps Research Institute, La Jolla, California, USA. [7]Division of Infectious Diseases, Department of Medicine, University of British Columbia, Vancouver, Canada. [8]Kyowa Hakko Kirin California Inc, La Jolla, California, USA. [9]Department of Pediatrics and Skaggs School of Pharmacy & Pharmaceutical Sciences, University of California, San Diego, La Jolla, California, USA. [10]Department of Applied Material and Life Science, College of Engineering, Kanto Gakuin University, Yokohama, Japan. [11]Department of Infection, Immunity and Inflammation, University of Leicester, Leicester, UK. [12]Department of Medical Microbiology, Mycology and Immunology, Tohoku University Graduate School of Medicine, Sendai, Japan. [13]These authors contributed equally to this work. Correspondence should be addressed to M.K. (mitch@liai.org).

Received 21 December 2010; accepted 27 July 2011; published online 4 September 2011; doi:10.1038/ni.2096

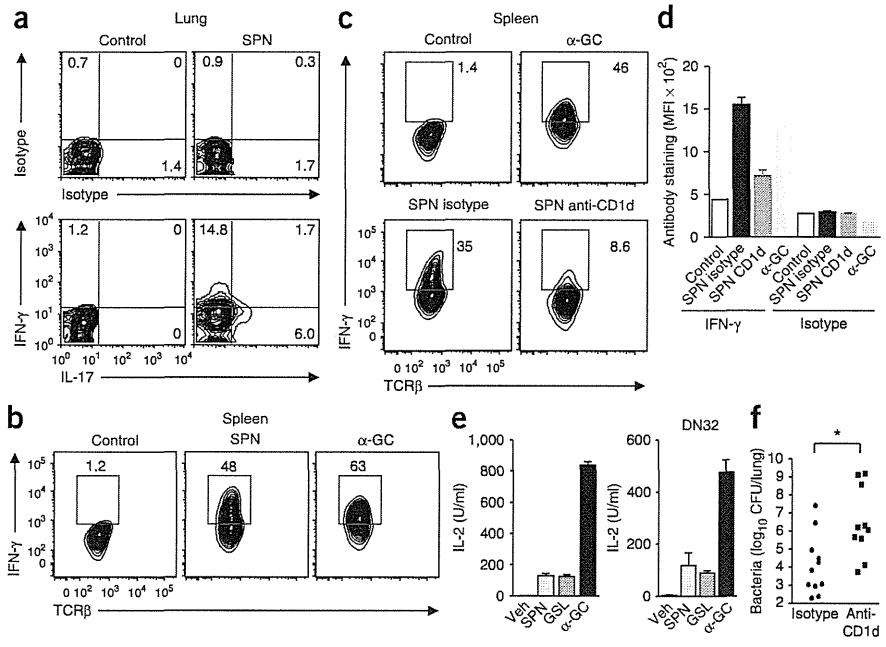


**Figure 1** CD1d-dependent cytokine production by $V_\alpha14i$ NKT cells. (**a**) Expression of intracellular IFN-γ and IL-17 by $CD19^-$ lung mononuclear cells positive for α-GalCer-loaded CD1d tetramer, measured in uninfected mice (Control) or 13 h after intratracheal infection with *S. pneumoniae* (SPN; cells combined from at least five mice per condition). Isotype, isotype-matched control antibody. Numbers in quadrants indicate percent cells in each throughout. (**b**) Expression of intracellular IFN-γ by tetramer-positive $CD19^-$ spleen cells from an uninfected mouse (Control), a mouse 6 h after intravenous infection with *S. pneumoniae* (SPN; $n = 3$) or a mouse injected with α-GalCer 1.5 h before tissue collection (α-GC). (**c**,**d**) Expression of intracellular IFN-γ by tetramer-positive $CD19^-$ spleen cells from an uninfected mouse or a mouse injected with α-GalCer as in **b**, and from mice treated with anti-CD1d (SPN anti-CD1d) or isotype-matched control antibody (SPN isotype) and infected intravenously with *S. pneumoniae*, assessed 6 h later ($n = 3$ per group). MFI, mean fluorescence intensity. Numbers adjacent to outlined areas (**b**,**c**) indicate percent IFN-γ⁺TCRβ⁺ cells. (**e**) Enzyme-linked immunosorbent assay of IL-2 produced by $V_\alpha14i$ NKT cell hybridoma clones 1.2 and DN32 cultured with $CD11c^+$ cells from spleens of mice injected with buffer containing Tween 20 vehicle (Veh), infected 16 h earlier with *S. pneumoniae* (SPN), injected 16 h earlier with synthetic glycosphingolipid antigen from *Sphingomonas* bacteria (GSL) or injected with α-GalCer (α-GC). (**f**) Bacterial burden in lungs of mice treated with anti-CD1d or isotype-matched control antibody (immunoglobulin G), assessed 3 d after infection with *S. pneumoniae*. Each symbol represents an individual mouse. CFU, colony-forming units. $^*P < 0.05$ (Mann-Whitney test). Data are representative of at least two experiments with similar results (**a**–**d**; mean and s.d. in **d**) or two independent experiments (**e**; mean and s.d. of triplicate wells) or are from two independent experiments (**f**).

factor and production of the chemokine CXCL2 (MIP-2), leading to enhanced recruitment of neutrophils to the lung[16].

Here we demonstrate CD1d-dependent activation of $V_\alpha14i$ NKT cells *in vivo* after infection with *S. pneumoniae*, which indicates antigen-dependent activation of these cells. Furthermore, we identify the unique structures of glycolipids from *S. pneumoniae* and another Gram-positive pathogen, group B *Streptococcus*, which were recognized by the *i*NKT cell TCR. Our data demonstrate a requirement in these glycolipid antigens for a fatty acid that is infrequent in mammalian cells. Additionally, we determine the unique binding mode of these antigens to mouse CD1d by solving the crystal structure of the antigen-CD1d complex. We propose that the *i*NKT cell TCR is a particularly useful and conserved specificity in part because it recognizes glycolipids from important pathogens that cause invasive, rapid and potentially lethal infections.

## RESULTS

### $V_\alpha14i$ NKT cells produce IFN-γ after infection

The protective effect of $V_\alpha14i$ NKT cells after infection with *S. pneumoniae* is dependent on the ability of mononuclear cells to produce IFN-γ[16], but several cell types can produce IFN-γ, and its production by activated $V_\alpha14i$ NKT cells has not been demonstrated directly. We therefore determined if $V_\alpha14i$ NKT cells synthesize cytokines after intratracheal infection of mice with *S. pneumoniae*. At 13 h after infection with *S. pneumoniae*, we stained lung mononuclear cells with CD1d tetramers loaded with α-galactosylceramide (α-GalCer), which specifically detect *i*NKT cells, then analyzed the stained cells for intracellular cytokines immediately after isolation, without restimulation or treatment with brefeldin A. A substantial frequency of $V_\alpha14i$ NKT cells in the lungs had intracellular IFN-γ or interleukin 17 (IL-17) at 13 h after infection (**Fig. 1a** and **Supplementary Fig. 1a**). We also detected intracellular IFN-γ in $V_\alpha14i$ NKT cells in the spleen at 6 h after intravenous infection with *S. pneumoniae* (**Fig. 1b** and **Supplementary Fig. 1b**), although under these circumstances intracellular IL-17 was not detectable (data not shown). Similarly, we also detected intracellular IFN-γ in $V_\alpha14i$ NKT cells in the liver after systemic infection (data not shown).

$V_\alpha14i$ NKT cells can be activated by cytokines, particularly IL-12, even in the absence of antigen presentation by CD1d and engagement of the TCR[8,9,17]. Therefore, we sought evidence that a TCR-dependent response was contributing to the activation of the $V_\alpha14i$ NKT cells after infection. To achieve this, we injected a blocking antibody to CD1d (anti-CD1d) into infected mice. The frequency of IFN-γ⁺ tetramer-positive cells was much lower after blockade of CD1d (**Fig. 1c**,**d** and **Supplementary Fig. 1c**), which indicated involvement of TCR recognition in the activation of the $V_\alpha14i$ NKT cells *in vivo* in the early phases of *S. pneumoniae* infection. To confirm the idea that an antigen that engages the $V_\alpha14i$ NKT cell TCR is formed after infection, we purified $CD11c^+$ cells from spleen of *S. pneumoniae*–infected mice. We then analyzed these antigen-presenting cells (APCs) for their ability to activate $V_\alpha14i$ NKT cell hybridomas for IL-2 release, a response that is dependent only on TCR engagement. Although $V_\alpha14i$ NKT cell hybridomas were not responsive to IL-12 or lipopolysaccharide (data not shown), we found that APCs stimulated the release of IL-2 from $V_\alpha14i$ NKT cell hybridomas and that they were as effective as APCs preloaded with synthetic glycosphingolipid (GSL) antigen from *Sphingomonas* bacteria (**Fig. 1e**). To determine if CD1d-dependent activation of $V_\alpha14i$ NKT cells also has a role in clearance of bacteria, we treated mice with monoclonal antibody (mAb) to CD1d or isotype-matched control antibody and infected the mice intratracheally with *S. pneumoniae*, then counted bacteria in the lungs at 3 d after infection. Injection of mAb to CD1d resulted in significantly more bacterial colonies (**Fig. 1f**).

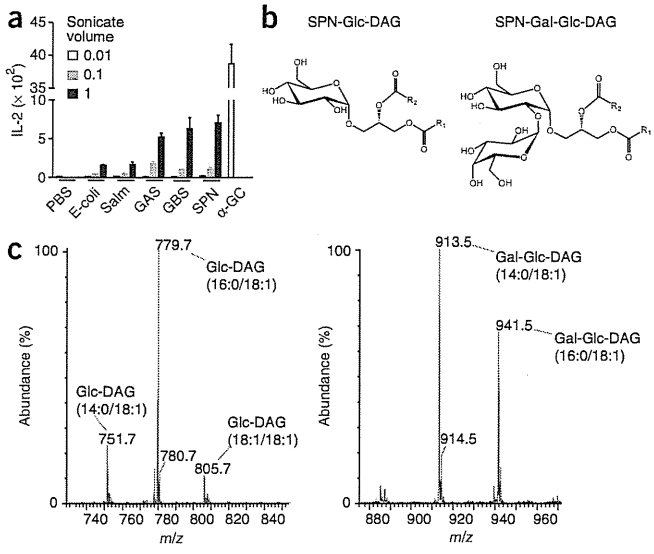


**Figure 2** Structure of *S. pneumoniae* glycolipids. (**a**) Enzyme-linked immunosorbent assay of IL-2 in supernatants of $V_\alpha14i$ NKT cell hybridoma 1.2 assessed in an APC-free assay of PBS alone, *E. coli* (E-coli), *S. typhimurium* (Salm), group A *Streptococcus* (GAS), group B *Streptococcus* (GBS), *S. pneumoniae* (SPN) or α-GalCer (α-GC; 5 ng/well). The sonicate volumes 0.01, 0.1 and 1 (key) are equivalent to $1 \times 10^6$, $1 \times 10^7$ and $1 \times 10^8$ bacteria per well, respectively. (**b**) Structure of *S. pneumoniae* glycolipids SPN-Glc-DAG (left) and SPN-Gal-Glc-DAG (right). (**c**) Electrospray-ionization mass spectrometry analysis of SPN-Glc-DAG (left) and SPN-Gal-Glc-DAG (right); fatty acid composition is in parentheses. *m/z*, mass/charge. Data are representative of two experiments (**a**; mean and s.e.m. of triplicate wells) or three experiments (**c**).

In sum, these data suggest that infection of DCs with *S. pneumoniae in vivo* leads to the generation of an antigen that can stimulate the TCR of $V_\alpha14i$ NKT cells and that antigen recognition is important in the clearance of *S. pneumoniae*.

### $V_\alpha14i$ NKT cell hybridomas respond to bacterial sonicates

Because *i*NKT cells can be activated by either self or foreign antigens[2], we determined if *S. pneumoniae* contain compounds that can stimulate the *i*NKT cell TCR. We prepared sonicates from a *S. pneumoniae* clinical isolate whose clearance is impaired in $V_\alpha14i$ NKT cell–deficient mice[15]. We incubated those bacterial sonicates in microwell plates coated with soluble mouse CD1d molecules. We observed dose-dependent IL-2 responses to the *S. pneumoniae* sonicates with two $V_\alpha14i$ NKT cell hybridomas with different $V_\beta8.2$ rearrangements (**Fig. 2a** and **Supplementary Fig. 2a**) and found that the response was inhibited by mAb to CD1d (**Supplementary Fig. 2b**). A CD1d-reactive hybridoma that does not bear the $V_\alpha14i$ TCR and does not recognize α-GalCer[18] did not respond to either bacterial sonicate (**Supplementary Fig. 2c**).

We compared those *S. pneumoniae* sonicates with ones prepared from several other bacteria, including important Gram-positive pathogens such as group A *Streptococcus*, which is estimated to cause over 500 million cases of pharyngitis and 600,000 invasive infections annually worldwide[19], and group B *Streptococcus*, the leading cause of life-threatening bacterial infections such as sepsis and meningitis in newborn humans[20]. When tested in the CD1d-coated-plate assay, sonicates of group A *Streptococcus* and group B *Streptococcus* also reproducibly induced the release of IL-2 from $V_\alpha14i$ NKT cell hybridomas. The Gram-negative bacteria *Escherichia coli* and *Salmonella typhimurium* are widely believed not to have glycolipid antigens for *i*NKT cells[11,17], and they produced much weaker responses, although in some assays *E. coli* sonicates produced completely negative results (**Fig. 2a** and data not shown). On the basis of these results, we cannot exclude the possibility that there is a weak antigen in *S. typhimurium* and perhaps in *E. coli* as well, but these sonicates did have less stimulatory activity.

### Structure of microbial glycolipids

We prepared crude lipid extracts from a panel of Gram-positive strains of clinical origin, including *S. pneumoniae* strains of serotypes 3, 12 and 17, a group B *Streptococcus* serotype IA strain, and a strain of the Gram-positive zoonotic pathogen *Streptococcus suis*. We fractioned lipids from these bacteria as described[21] and analyzed them by electrospray mass spectrometry, one- and two-dimensional nuclear magnetic resonance and gas chromatography–mass spectrometry (additional analysis details, **Supplementary Figs. 3–7**). We detected two main fractions of *S. pneumoniae* glycolipids. One had a single glucose sugar α-linked to diacylglycerol (DAG; 1,2-di-*O*-acyl-(α-glucopyranosyl)-(1→3)-glycerol) (called 'SPN-Glc-DAG' here; **Fig. 2b**). The second fraction was identical except it had a disaccharide moiety attached to the DAG, with galactose (Gal) α1→2 linked to the glucose sugar, resulting in (α-galactopyranosyl)-(1→2)-(α-glucopyranosyl)-(1→3)-glycerol) (called 'SPN-Gal-Glc-DAG' here; **Fig. 2b**). Analysis of SPN-Glc-DAG by electrospray mass spectrometry identified two main fatty acids: hexadecanoic acid ($C_{16:0}$) and octadecenoic acid ($C_{18:1}$; **Fig. 2c**). We confirmed that composition by gas chromatography–mass spectrometry analysis of fatty acid methyl esters (data not shown). We found the same fatty acids in disaccharide-containing SPN-Gal-Glc-DAG, but this glycolipid also had a substantial amount of tetradecanoic acid ($C_{14:0}$). Notably, we identified the structure of the octadecenoic acid as *cis*-vaccenic (octadecen-11-oic acid or $C_{18:1}$(n-7)), which has an unsaturated bond between the carbons at positions 11 and 12 (**Supplementary Fig. 5a**). Oleic acid, the more common $C_{18:1}$ fatty acid in mammalian cells[22], also present in the *Borrelia* DAG antigen, has a *cis* unsaturated bond between the carbons at positions 9 and 10 ($C_{18:1}$(n-9)). The group B *Streptococcus* DAG glycolipids did not differ from those obtained from *S. pneumoniae*, including the presence of vaccenic acid. One of the main glycolipids purified had an α-linked glucose monosaccharide (called 'GBS-Glc-DAG' here). As in *S. pneumoniae*, the other main chemical species had a disaccharide, but with two glucose sugars (Glc α1→2 Glc); we call this compound (α-glucopyranosyl)-(1→2)-(α-glucopyranosyl)-(1→3)-glycerol) (called 'GBS-Glc-Glc-DAG' here). Finally, the DAG glycolipid from *S. suis* had a monosaccharide with α-linked mannose. It is noteworthy that glucosylated DAG glycolipids are not found only in pathogens. We also analyzed the glycolipid content of a Gram-positive commensal organism, *Lactobacillus casei*, which had similar DAG glycolipids with α-linked glucose (data not shown).

### Microbial glycolipids stimulate $V_\alpha14i$ NKT cell hybridomas

To determine if the purified glycolipids were able to stimulate *i*NKT cells, we cultured $V_\alpha14i$ NKT cell hybridomas with A20 mouse B lymphoma cells transfected to express CD1d. $CD1d^+$ cells incubated with SPN-Glc-DAG or SPN-Gal-Glc-DAG induced CD1d-dependent release of IL-2 from the hybridomas (**Fig. 3a** and **Supplementary Fig. 8a**). To confirm that the purified *S. pneumoniae* glycolipids stimulated the invariant TCR of $V_\alpha14i$ NKT cells, we also tested them in the CD1d-coated-plate assay. *S. pneumoniae* glycolipids stimulated the release of IL-2 from all four $V_\alpha14i$ NKT cell hybridomas tested when added to CD1d-coated plates (**Fig. 3b**, **Supplementary Fig. 8b** and data

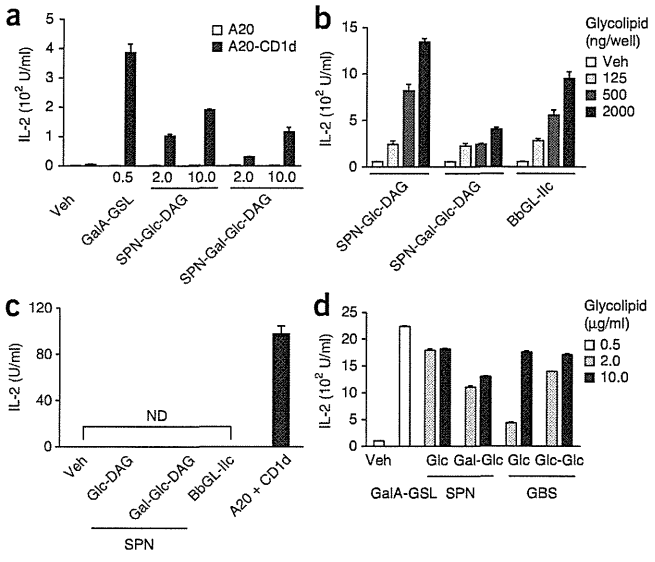


**Figure 3** Microbial glycolipids stimulate $V_\alpha14i$ NKT cells *in vitro*. (**a**) Release of IL-2 from cells of the $V_\alpha14i$ NKT cell hybridoma 1.2 cultured with A20 cells (A20) or A20 cells transfected to express mouse CD1d (A20-CD1d), pulsed for 20 h with buffer containing Tween 20 (vehicle), *Sphingomonas* GalA-GSL, SPN-Glc-DAG or SPN-Gal-Glc-DAG at various concentrations (horizontal axis; in μg/ml). (**b**) Release of IL-2 from cells of $V_\alpha14i$ NKT cell hybridoma 1.2 cultured for 20 h in mouse CD1d–coated wells with SPN-Glc-DAG, SPN-Gal-Glc-DAG or BbGL-IIc at various concentrations (key). (**c**) Release of IL-2 from cells of the non-$V_\alpha14$-expressing but CD1d-reactive hybridoma 19 in wells coated with CD1d, cultured with Tween 20 (vehicle) alone, SPN-Glc-DAG, SPN-Gal-Glc-DAG or BbGL-IIc (2,000 ng/well) or self antigen presented by A20 cells transfected to express mouse CD1d. ND, not detected. (**d**) Release of IL-2 from cells of the $V_\alpha14i$ NKT hybridoma 1.2 cultured with A20 cells, transfected to express mouse CD1d and pulsed with buffer containing Tween 20 (vehicle), *Sphingomonas* GalA-GSL, SPN-Glc-DAG (Glc), SPN-Gal-Glc-DAG (Gal-Glc), GBS-Glc-DAG (Glc) or GBS-Glc-Glc-DAG (Glc-Glc) at various concentrations (key). Data are representative of at least three (**a**,**b**,**d**) or two (**c**) experiments (mean and s.e.m. of triplicate wells).

not shown). In the coated-plate assay, the disaccharide-containing SPN-Gal-Glc-DAG stimulated weaker responses (**Fig. 3b**). On the basis of published work[23], we predicted these compounds might require lysosomal processing to generate a stimulatory monosaccharide antigen. The diminished responses to SPN-Gal-Glc-DAG were consistent with our prediction, and the residual response could have been due to contaminating monosaccharide. In agreement with the results obtained with the whole bacterial sonicates, none of these purified glycolipids stimulated two CD1d-reactive but non-$V_\alpha14i$ NKT cell hybridomas (**Fig. 3c** and data not shown), which demonstrated specific activation of T cells expressing the invariant TCR. Furthermore, GBS-Glc-DAG, GBS-Glc-Glc-DAG and the commensal-derived Glc-DAG of *L. casei* also stimulated $V_\alpha14i$ NKT cell hybridomas when cultured with $CD1d^+$ A20 cells pulsed with these compounds (**Fig. 3d** and **Supplementary Fig. 9a**,**b**).

It has been shown that GSL antigens containing α-linked glucose and galactose are antigenic, whereas those containing α-linked mannose are not[24]. The DAG lipid from *S. suis* containing α-linked mannose was not antigenic (**Supplementary Fig. 9c**). These data on DAG antigens suggest that the recognition of α-linked sugars in the DAG bacterial antigens is similar to the well-characterized recognition of the α-linked carbohydrates in GSLs. Consistent with that, elucidation of the trimolecular structures of the invariant TCR bound to complexes of mouse CD1d with a *Sphingomonas* GSL or a *Borrelia* DAG antigen indicates a similar binding mode for the TCR[25].

### Glycolipids stimulate $V_\alpha14i$ NKT cells *in vivo*

We determined if purified *S. pneumoniae* glycolipids were able to stimulate $V_\alpha14i$ NKT cells *in vivo*. We pulsed bone marrow–derived dendritic cells (DCs) with SPN-Glc-DAG, the disaccharide SPN-Gal-Glc-DAG or a synthetic version of the natural *Sphingomonas* galacturonic acid–containing GSL (GalA-GSL)[10] and transferred the cells into C57BL/6 mice; 14 h later, we analyzed activation of $V_\alpha14i$ NKT cells in liver and spleen. As a positive control, we transferred DCs pulsed with α-GalCer, the highly potent synthetic GSL antigen similar to the *Sphingomonas* antigens[10,11]. We analyzed cells that stained with α-GalCer-loaded CD1d tetramers for their expression of activation markers by flow cytometry. The expression of CD25 and CD69 on CD1d tetramer–positive cells was higher in mice treated with DCs pulsed with SPN-Glc-DAG than in mice treated with vehicle-pulsed DCs (**Fig. 4a** and **Supplementary Fig. 10a**). SPN-Gal-Glc-DAG also induced higher expression of CD25 and CD69, although to a lesser extent (**Fig. 4a** and **Supplementary Fig. 10a**). SPN-Glc-DAG induced intracellular expression of IFN-γ by most $V_\alpha14i$ NKT cells when they were analyzed immediately after isolation, equivalent to that induced by α-GalCer (**Fig. 4b**), which indicated that most $V_\alpha14i$ NKT cells responded to this antigen. We note that to obtain an optimal response, we incubated the DCs with more SPN-Glc-DAG than α-GalCer. We also observed intracellular IL-4 and tumor necrosis factor in activated liver $V_\alpha14i$ NKT cells, albeit on a smaller percentage of cells, but we did not detect IL-17 (**Supplementary Fig. 10b**,**c**). We observed lower cytokine responses in response to the disaccharide compound (**Fig. 4b**), in agreement with the lower induction of expression of activation markers. Purified glycolipid from group B *Streptococcus* induced a similar response *in vivo* (**Fig. 4c** and **Supplementary Fig. 11**), reflective of its essentially identical structure.

Activation of *i*NKT cells can be achieved in the absence of foreign glycolipid antigens by endogenous antigen(s) presented by CD1d and/or by inflammatory cytokines, such as IL-12, which are produced by APCs stimulated with Toll-like receptor (TLR) ligands[8,17]. At a relatively early time (4 h after the transfer of SPN-Glc-DAG–pulsed DCs into mice), many of the cytokine-producing $V_\alpha14i$ NKT cells were positive for both intracellular IFN-γ and IL-4 (**Supplementary Fig. 12a**,**b**) when analyzed immediately after isolation. This is consistent with TCR-mediated activation of these cells because IL-4 production has not been observed in $V_\alpha14i$ NKT cells stimulated only indirectly by inflammatory cytokines such as IL-12 (refs. 8,17). To confirm that TLR-mediated activation of APCs is not required for the activation of $V_\alpha14i$ NKT cells induced by *S. pneumoniae* glycolipids, we pulsed DCs from TLR signaling–defective (*Myd88*$^{-/-}$*Trif*$^{Lps2/Lps2}$) mice with SPN-Glc-DAG or SPN-Gal-Glc-DAG and transferred the DCs into *Myd88*$^{-/-}$ mice or wild-type mice, then stained $V_\alpha14i$ NKT cells for intracellular cytokines. DCs from *Myd88*$^{-/-}$*Trif*$^{Lps2/Lps2}$ mice were able to stimulate equal production of IFN-γ and IL-4 by $V_\alpha14i$ NKT cells from recipient *Myd88*$^{-/-}$ mice or wild-type mice (**Fig. 4d** and **Supplementary Fig. 13**). Furthermore, the magnitude of the response to TLR signaling–defective DCs was similar to the response obtained when both donor DCs and recipient mice were wild-type. Consistent with that, IL-12-deficient DCs that had been pulsed with SPN-Glc-DAG also were still able to induce cytokines from $V_\alpha14i$ NKT cells when transferred into IL-12-deficient mice (**Fig. 4e** and **Supplementary Fig. 14a**,**b**). Therefore, the *in vivo* activation of $V_\alpha14i$ NKT cells by the purified glycolipids was due to TCR-dependent activation by microbial glycolipid antigens and did not require activation of the innate immune response and IL-12.

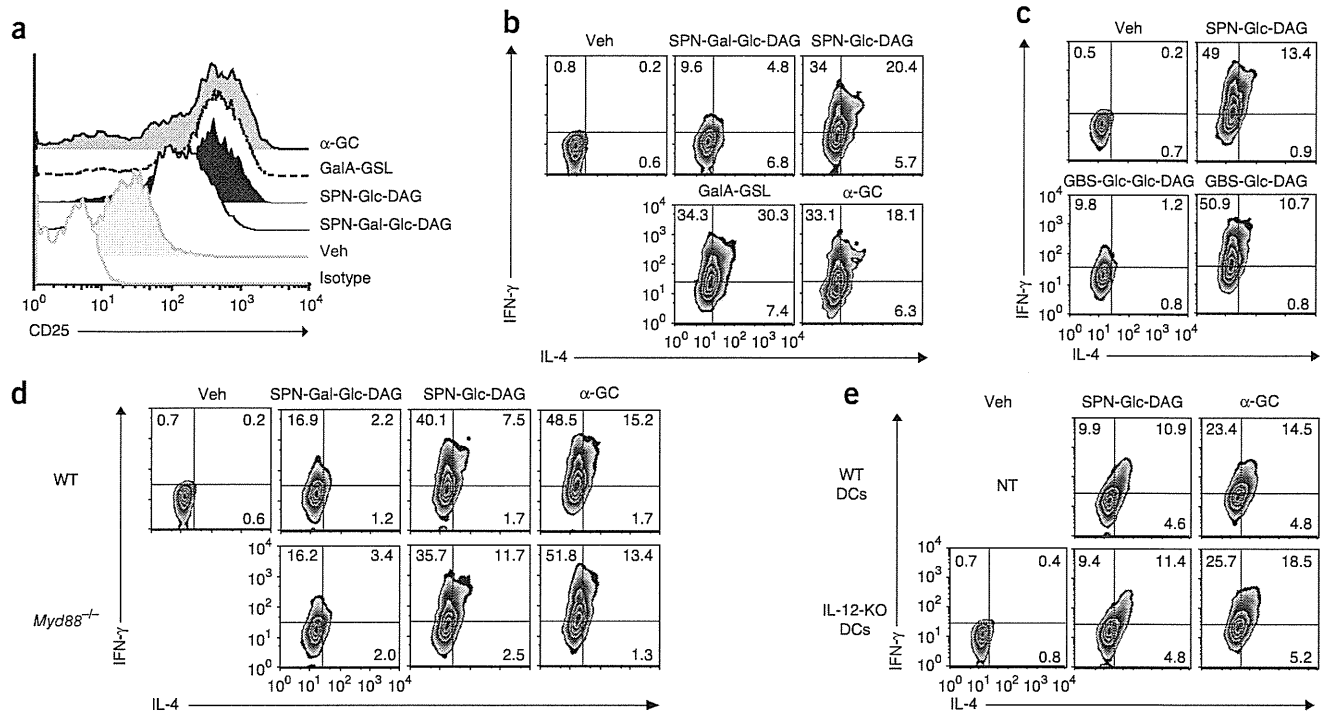


**Figure 4** *In vivo* stimulation of $V_\alpha 14i$ NKT cells by purified glycolipids. (**a**,**b**) Expression of CD25 (**a**) and intracellular IFN-γ and IL-4 (**b**) by tetramer-positive $V_\alpha 14i$ NKT cells (liver mononuclear cells) obtained from mice 14 h after transfer of DCs pulsed with α-GalCer (0.1 μg/ml), *Sphingomonas* GalA-GSL (10 μg/ml), SPN-Glc-DAG (20 μg/ml), SPN-Gal-Glc-DAG (20 μg/ml) or vehicle alone. (**c**) Expression of intracellular IFN-γ and IL-4 by tetramer-positive liver mononuclear cells obtained from mice 14 h after transfer of DCs pulsed with vehicle, SPN-Glc-DAG, GBS-Glc-DAG or GBS-Glc-Glc-DAG (20 μg/ml). (**d**) Intracellular expression of IFN-γ and IL-4 by liver mononuclear cells (positive for CD1d tetramer loaded with α-GalCer) obtained from wild-type or *Myd88*$^{-/-}$ mice 14 h after transfer of *Myd88*$^{-/-}$ *Trif*$^{Lps2/Lps2}$ DCs pulsed with vehicle, SPN-Gal-Glc-DAG (20 μg/ml), SPN-Glc-DAG (20 μg/ml) or α-GalCer (0.1 μg/ml). (**e**) Expression of intracellular IFN-γ and IL-4 by tetramer-positive liver mononuclear cells obtained from IL-12p35-deficient mice 4 h after transfer of wild-type or IL-12p35-deficient (IL-12-KO) DCs pulsed with vehicle, SPN-Glc-DAG (20 μg/ml) or α-GalCer (0.1 μg/ml). NT, not tested. Data are representative of at least two independent experiments with similar results ($n = 3$ mice per group, except $n = 2$ mice for α-GalCer in **d**).

Although activation of $V_\alpha 14i$ NKT cells by glycolipid-pulsed APCs did not depend on IL-12, activation after *S. pneumoniae* infection did. In agreement with published work[9], the induction of CD69 expression on $V_\alpha 14i$ NKT cells was the same in wild-type and IL-12-deficient mice after infection with *S. pneumoniae*; however, IFN-γ production by $V_\alpha 14i$ NKT cells was much lower in mice deficient in the p35 subunit of IL-12 (**Supplementary Fig. 15**).

### Stimulation of *i*NKT cells by synthetic Glc-DAG antigens

We tested synthetic compounds to verify the identity of the purified material that activated *i*NKT cells. We synthesized versions of SPN-Glc-DAG containing vaccenic acid in the *sn*-1 position (Glc-DAG-s1) or the *sn*-2 position (Glc-DAG-s2), which reflects the structure of the natural antigen, or in both positions (Glc-DAG-s3), with hexadecanoic acid in the remaining position for Glc-DAG-s1 and Glc-DAG-s2 (**Table 1**). To further assess the importance of vaccenic acid, we also tested two compounds with a $C_{18:1}$ oleic acid. In the hybridoma-stimulation assay with APCs transfected to express CD1d, the synthetic version of the naturally occurring antigen, Glc-DAG-s2, was the only compound that induced considerable release of IL-2 (**Supplementary Fig. 16a**). Compounds with vaccenic acid in the *sn*-1 position or linked to both the *sn*-1 and *sn*-2 glycerol positions were ineffective, as were compounds with oleic acid. To test the response of $V_\alpha 14i$ NKT cells *in vivo*, we loaded bone marrow DCs with each of the synthetic compounds and injected them into mice, then analyzed cells from the recipient mice immediately after isolation, as with the purified material. In this *in vivo* stimulation assay, we observed a degree of selectivity similar to of the hybridoma assay noted above (**Supplementary Fig. 16a**). Only Glc-DAG-s2 induced surface upregulation of the activation markers CD25 (**Fig. 5a**) and CD69 (**Supplementary Fig. 16b**) and intracellular cytokines (**Fig. 5b** and **Supplementary Fig. 16c**).

In agreement with the results indicating that the purified glycolipid did not activate the innate immune system, synthetic Glc-DAG-s2 did not stimulate bone marrow–derived dendritic cells to increase their surface expression of CD1d and costimulatory molecules, including CD40 and CD80, whereas lipopolysaccharide induced the upregulation of these molecules (**Supplementary Fig. 17a**). Also, APCs pulsed with Glc-DAG-s2 did not increase the autoreactivity of a CD1d-reactive hybridoma that does not express the invariant TCR (**Supplementary Fig. 17b**). Furthermore, as with the purified compounds, cytokine release was not dependent on secretion of IL-12, which confirmed the requirement for TCR-dependent activation (data not shown). Lipopolysaccharide did cause slightly more reactivity of the hybridoma lacking the invariant TCR (**Supplementary Fig. 17b**), although it did not do so for a $V_\alpha 14i$ NKT cell hybridoma. We attribute this result to augmented CD1d expression, although more synthesis of the self antigen for this cell is also possible.

Mouse and human *i*NKT cells tend to recognize the same glycolipids presented by CD1d[1,2,6,7], although differences in the requirement for particular fatty acids in the *B. burgdorferi* DAG antigens have been reported[12,26]. We therefore tested several human $V_\alpha 24i$ NKT cell lines, which had been expanded with α-GalCer and IL-2, for reactivity

**Table 1 Fatty acids in synthetic variants of Glc-DAG**

| Glycolipid | $R_1$ (*sn*-1) | $R_2$ (*sn*-2) |
|---|---|---|
| Glc-DAG-s1 | $C_{18:1}$(n-7) | $C_{16:0}$ |
| Glc-DAG-s2 | $C_{16:0}$ | $C_{18:1}$(n-7) |
| Glc-DAG-s3 | $C_{18:1}$(n-7) | $C_{18:1}$(n-7) |
| Glc-DAG-s4 | $C_{18:1}$(n-9) | $C_{16:0}$ |
| Glc-DAG-s5 | $C_{16:0}$ | $C_{18:1}$(n-9) |

to the purified and synthetic Glc-DAG glycolipids. $V_\alpha$24*i* NKT cells secreted IFN-γ when cultured with the purified material and, like mouse $V_\alpha$14*i* NKT cells, they responded selectively to Glc-DAG-s2 (with vaccenic acid in the *sn*-2 position; **Fig. 5c**). We obtained similar results with four other $V_\alpha$24*i* NKT cell lines (data not shown) and for the release of IL-4 (**Supplementary Fig. 18**).

### The CD1d-binding mode of *S. pneumoniae* glycolipid

Although the α-glucosyl ceramide isomer of α-GalCer differs from α-GalCer only by the orientation of the 4′ OH group of the hexose sugar, it is a weaker antigen[24], with approximately 10% of the affinity for the TCR[27,28]. Despite that, glucose-containing antigens such as Glc-DAG-s2 were approximately as potent as the galactose-containing *B. burgdorferi* DAG antigen BbGL-IIc, working slightly better on CD1d-coated plates (**Fig. 3** and **Supplementary Fig. 8b**) but slightly more weakly with APCs (**Supplementary Figs. 9b** and **16a**). A compound containing an α-linked glucose sugar was not antigenic, however, when linked to the same fatty acids as those in the galactose-containing *B. burgdorferi* antigen, with $C_{18:1}$ oleic acid in the *sn*-1 position and $C_{16:0}$ palmitic acid in *sn*-2 (Glc-DAG-s4; **Fig. 5** and **Supplementary Figs. 16** and **18**). Furthermore, a galactose containing DAG antigens with the same *S. pneumoniae* fatty acids was a less potent stimulator of *i*NKT cells (data not shown). Our data therefore indicate an intricate interaction between the lipid and sugar, with stringent requirements for both in determining antigenic potency, at least for the DAG-containing glycolipid antigens.

Given the requirements for a glucose sugar and an unusual fatty acid, to understand the basis for the activity of Glc-DAG-s2, we determined the crystal structure of the complex of Glc-DAG-s2 with mouse CD1d at a resolution of 1.7Å (**Fig. 6** and **Supplementary Table 1**). The data showed that the uncommon vaccenic acid at the *sn*-2 position of Glc-DAG-s2 was bound in the A′ pocket of mouse CD1d, encircling the A′ pole in a clockwise orientation. This was in contrast to most other CD1d-glycolipid structures, which have a counterclockwise orientation of a hydrophobic chain in the A′ pocket[29,30]. The *sn*-1 linked palmitic acid was bound in the F′ pocket while leaving the *sn*-3 linked α-anomeric glucose exposed for recognition by T cells (**Fig. 6a,b**). The opposite binding orientation, with the *sn*-1 and *sn*-2 chains in the A′ and F′ pockets, respectively, was not supported by the electron density in the region of the glycerol moiety and the polar head group (**Fig. 6a**). However, we observed poor electron density at the end of the *sn-1* chain, most probably the result of the various conformations the acyl chain can adopt in this portion of the F′ pocket, as described for several other mouse CD1d ligands[30]. The binding mode of Glc-DAG-s2, probably influenced by the position of the *cis*-unsaturation of the vaccenic acid, differed from the binding of the other known bacterial DAG antigen, BbGL-IIc of *B. burgdorferi*, which has the *sn*-2 fatty acid in the F′ pocket and the *sn*-1 $C_{18:1}$ oleic acid wound in a counterclockwise direction in the A′ pocket[26].

Notably, the position of the glucose head group in Glc-DAG-s2 mouse CD1d complexes was different from the position of the galactose in the complexes of α-GalCer with mouse CD1d (**Fig. 6c**), although it did resemble the position of the galactose in BbGL-IIc. Key contacts between Asp153 and the 2′-OH and 3′-OH groups of the galactose of α-GalCer were not conserved but, similar to the structure of other DAG antigens, instead the sugar of Glc-DAG-s2 was slightly more upright in the binding groove and farther from Asp153 (**Fig. 6c**), probably positioned in this way as a result of its different lipid backbone. A 60° counterclockwise rotation of the glucose relative to the position of α-GalCer, when viewed from above the carbohydrate, brought the 2′ OH of the glucose in proximity to Arg79, where it formed the only hydrogen-bond interaction directly with a mouse CD1d amino acid. A further $H_2O$-mediated hydrogen bond was formed between the 6′ OH of glucose and the backbone oxygen of the *sn*-2-linked fatty acid with Thr159 of mouse CD1d. Overall, these few interactions between the glucose and mouse CD1d gave rise to only a weak electron density for the glucose head group, which suggested a more flexible and dynamic binding for Glc-DAG-s2. Furthermore, from the perspective of the TCR, the glucose moiety was shifted away from Asp153 and toward the α-helix amino acid Arg79, sitting more to the center of the binding groove and similar to the structure of BbGL-IIc, in contrast to the binding of α-GalCer to mouse CD1d, in which the galactose was in more intimate contact with Asp153 of the α2 helix (**Fig. 6c–f**). The position of the hexose sugar should be more unfavorable for

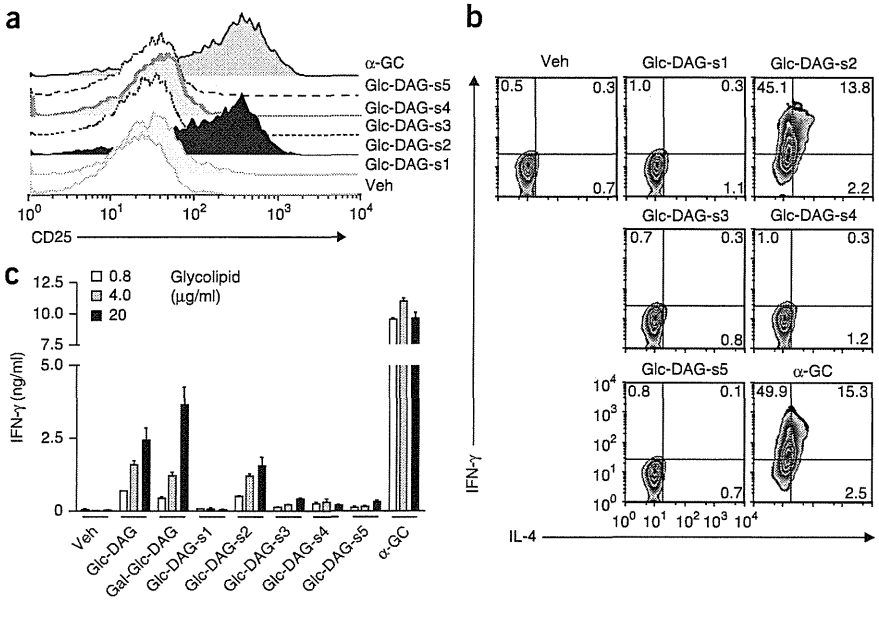


**Figure 5** Stringent requirement for vaccenic acid in the stimulation of *i*NKT cells. (**a**,**b**) Expression of CD25 (**a**) and intracellular IFN-γ and IL-4 (**b**) by tetramer-positive liver mononuclear cells obtained from mice ($n = 3$ per group) 14 h after transfer of DCs pulsed with α-GalCer (0.1 μg/ml), synthetic variants of Glc-DAG (Glc-DAG-s1 through Glc-DAG-s5 (fatty acid composition, **Table 1**); 20 μg/ml) or vehicle. (**c**) Secretion of IFN-γ by human $V_\alpha$24*i* NKT cell lines ($n = 5$) cultured for 24 h with human Hela cells transfected to express CD1d, in the presence of vehicle alone, purified glycolipids (Glc-DAG and Gal-Glc-DAG), synthetic glycolipids (Glc-DAG-s1 through Glc-DAG-s5) or α-GalCer. Data are representative of two independent experiments with similar results (**a**,**b**) or two experiments (**c**; mean and s.d. of triplicate wells).

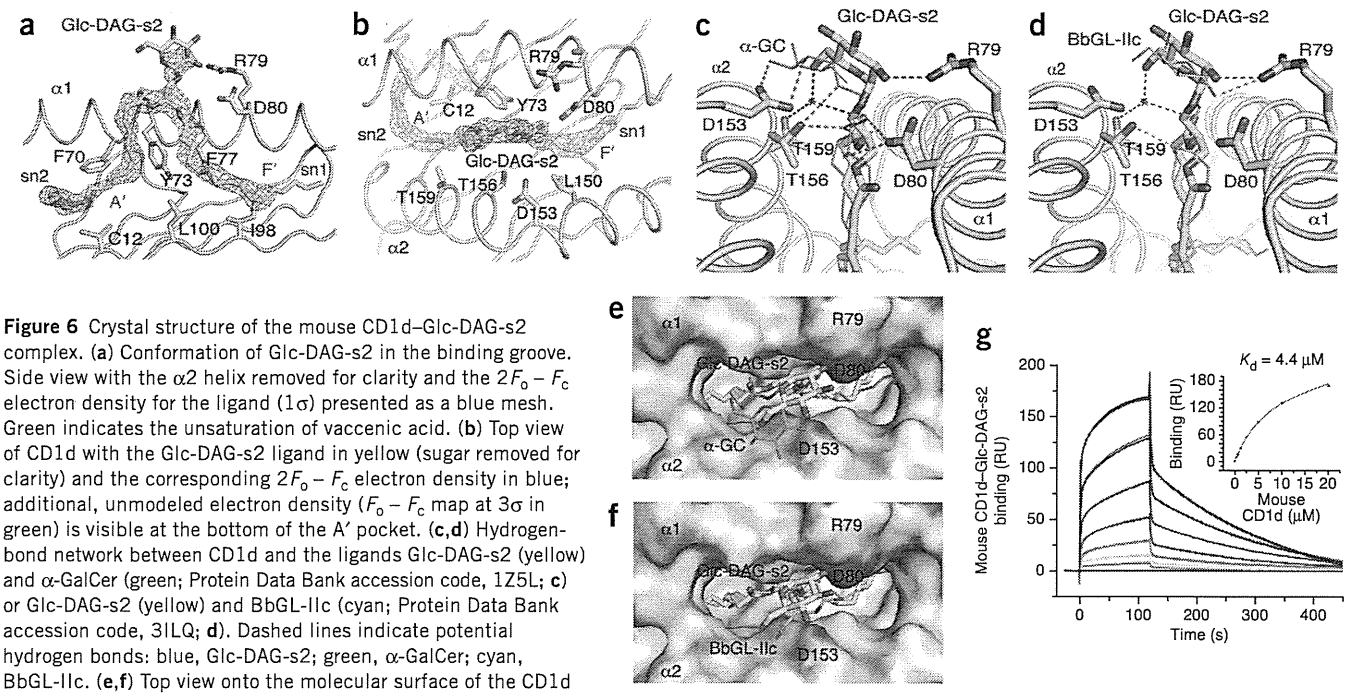


**Figure 6** Crystal structure of the mouse CD1d–Glc-DAG-s2 complex. (**a**) Conformation of Glc-DAG-s2 in the binding groove. Side view with the α2 helix removed for clarity and the $2F_o - F_c$ electron density for the ligand (1σ) presented as a blue mesh. Green indicates the unsaturation of vaccenic acid. (**b**) Top view of CD1d with the Glc-DAG-s2 ligand in yellow (sugar removed for clarity) and the corresponding $2F_o - F_c$ electron density in blue; additional, unmodeled electron density ($F_o - F_c$ map at 3σ in green) is visible at the bottom of the A′ pocket. (**c**,**d**) Hydrogen-bond network between CD1d and the ligands Glc-DAG-s2 (yellow) and α-GalCer (green; Protein Data Bank accession code, 1Z5L; **c**) or Glc-DAG-s2 (yellow) and BbGL-IIc (cyan; Protein Data Bank accession code, 3ILQ; **d**). Dashed lines indicate potential hydrogen bonds: blue, Glc-DAG-s2; green, α-GalCer; cyan, BbGL-IIc. (**e**,**f**) Top view onto the molecular surface of the CD1d binding pocket, including its electrostatic potentials: yellow, Glc-DAG-s2 ligand; green, α-GalCer (**e**); cyan, BbGL-IIc (**f**). (**g**) Binding response of mouse CD1d–Glc-DAG-s2 to immobilized $V_\alpha14V_\beta8.2$ TCR, measured by surface plasmon resonance and presented as response units (RU). Inset, binding of increasing concentrations (0.3125–20 μM) of the CD1d–DAG antigen complex.

the TCR for structures with a galactose sugar in α-linkage to the same *S. pneumoniae* DAG lipid, in which case the 4′ OH in the axial position would be tilted even more from the optimal position.

### Avid binding of TCRs to *S. pneumoniae* complexes with CD1d

Surface plasmon resonance binding studies with a refolded $V_\alpha14i$ NKT cell TCR supported the idea that the glucose sugar for this class of antigens gives rise to a relatively strong antigenic response similar to that of the *Borrelia* antigens with galactose sugars. The equilibrium dissociation constant for Glc-DAG-s2 was 4.4 ± 0.4 μM (mean ± s.d.), which was slightly better than that of the galactose-containing BbGL-IIc (6.2 μM)[26]. Binding to the TCR was slower (association rate constant, 1,380 ± 60 $M^{-1}s^{-1}$), and the dissociation was also much slower (dissociation rate constant, 0.00605 ± 0.0003 $s^{-1}$) than the binding and dissociation of BbGL-IIc (**Fig. 6g**). We conclude that the unique hydrophobic chains of the *S. pneumoniae* antigens contribute to the TCR epitope, despite being buried in the CD1d groove, because the orientation of lipid binding to the two pockets of mouse CD1d defines the position of the exposed sugar. Additionally, the altered orientation of the sugar probably permits glucose-containing antigens to be 'preferred' over galactose, unlike the use of either GSL antigens with ceramide lipids or *the B. burgdorferi* DAG antigens with $C_{18:1}$ oleic acids.

## DISCUSSION

Here we have shown that the TCR expressed by mouse and human *i*NKT cells recognized unique glycolipid antigens from *S. pneumoniae* and group B *Streptococcus*, which are among the most serious and widespread bacterial pathogens. Notably, the *i*NKT cell response to these glycolipids was conserved in humans. Published work has demonstrated that $V_\alpha14i$ NKT cells are important for host protection[15], and we have now demonstrated that $V_\alpha14i$ NKT cells produced IFN-γ and IL-17 rapidly *in vivo* in the lung after infection with *S. pneumoniae*. This *in vivo* cytokine synthesis was diminished by treatment with mAb to CD1d, and APCs from infected mice activated $V_\alpha14i$ NKT cell hybridomas to produce IL-2, a response that required TCR engagement. Together these results suggest that *i*NKT cells produce cytokines *in vivo* after infection with *S. pneumoniae* because of recognition of an antigen (or antigens) presented by CD1d. Additionally, in agreement with the greater susceptibility of Jα18-deficient mice[15] and CD1d-deficient mice[9] to infection with *S. pneumoniae*, treatment with mAb to CD1d resulted in a greater *S. pneumoniae* colony count in the lung. Therefore, these data suggest that not only is cytokine production by $V_\alpha14i$ NKT cells *in vivo* dependent on TCR engagement but the host-protective effects of $V_\alpha14i$ NKT cell activation are as well.

We cannot exclude the possibility, however, that some of the CD1d-dependent *in vivo* activation of *i*NKT cells was due to self antigens presented by CD1d. A published study has provided evidence suggesting that the predominant response of $V_\alpha14i$ NKT cells to bacterial infection, including infection with *S. pneumoniae*, is stimulated by IL-12 from activated APCs, leading to the secretion of IFN-γ but not of IL-4 by the $V_\alpha14i$ NKT cells[9]. Microbes known to have antigens and those probably lacking an antigen produce similar responses. This has led to the suggestion that antigen-independent or self antigen–dependent responses are probably dominant over responses to foreign antigen. IL-12 also can act in synergy with responses to relatively weak foreign antigens, and the TCR affinity for the DAG antigens is in the low micromolar range, whereas for α-GalCer it is in the low nanomolar range[26]. We also found that the *in vivo* response to *S. pneumoniae* was dominated by IFN-γ, although we detected IL-17 synthesis by lung $V_\alpha14i$ NKT cells, which probably reflected the greater presence of $V_\alpha14i$ NKT cells committed to IL-17 production there[31]. This is potentially important, given the reported role for IL-17 in the host response to *S. pneumoniae*[32].

It should be possible to distinguish the relative contributions of self and foreign antigens to the activation of $V_\alpha14i$ NKT cells by removing

the expression of either. However, the structures of the predominant self antigens remain controversial, and some published results suggest that they may be diverse[33]. On the microbial side, the results of targeted mutagenesis of the *S. pneumoniae* gene encoding the enzyme that links the glucose sugar to DAG suggest that inactivation of this gene is a lethal mutation. Similarly, group B *Streptococcus* strains with mutated genes encoding molecules involved in the synthesis of unsaturated fatty acids required supplementation with more than one type of fatty acid for their growth, which also apparently allowed the formation of antigens (J.L.V., S.D., S.U. and V.N., data not shown). Therefore, although we cannot unambiguously distinguish the contributions of self and microbial antigens to the CD1d-mediated activation of $V_\alpha 14i$ *i*NKT cells *in vivo*, it is likely that the antigens defined here, which had micromolar affinity for the invariant TCR once bound to CD1d, do make a contribution to the production of cytokines by $V_\alpha 14i$ NKT cells.

Published studies have identified glycosylated DAG antigens in *S. pneumoniae*[9,21], although the complete structures and their antigenic activity have not been determined[9]. The bacterial DAG lipid antigens we have defined here had an unusual *sn*-2-linked fatty acid. Because the aliphatic hydrocarbon chains were buried in the groove, their structure might be expected to be largely irrelevant in determining antigenic potency. However, our data have demonstrated that not only did the exposed sugar contribute to activation but also the microbial lipid made a critical contribution. We found that the position of a single unsaturated bond in vaccenic acid linked to the *sn*-2 position of the glycerol was an important feature for defining the potency of these glucose-containing antigens. Notably, vaccenic acid is uncommon in mammalian cells[22]. The carbohydrate portion, linked to the *sn*-3 position of DAG, is also of interest. It is either a glucose monosaccharide or a disaccharide with glucose linked to the DAG moiety. It was unexpected that glucose was favored as the sugar linked to DAG rather than galactose because this was not true in the context of other glycolipid antigens. We propose that because of the presence of vaccenic acid positioning the DAG antigen, SPN-Glc-DAG-s2 is presented by mouse CD1d in a position more tilted up away from CD1d and toward the TCR, so that the initial interaction of the TCR with a galactose-containing antigen, which contains an axial 4′ OH, may be disfavored. This is consistent with the slower TCR association we found for binding to Glc-DAG-s2 complexes with CD1d. It is likely, however, that after binding the antigen-CD1d complex, the TCR would flatten the orientation of the Glc-DAG-s2 sugar to maintain the conserved binding mode found for other antigens[25,28,33]. Regardless of the mechanism of antigen recognition, our work has established that there are interactions among the lipid, sugar and CD1d in forming an epitope, with stringent requirements for both the lipid and sugar structures. These stringent requirements suggest that a microbe could avoid activation of *i*NKT cells through subtle changes in the biosynthesis of either glycolipid component.

The ability of the *i*NKT cell TCR to recognize diverse antigens in a conserved manner has been referred to as 'pattern recognition'[34]. The original idea of pattern recognition referred to a microbe-associated molecular pattern, which is a structural feature of fundamental importance to microbes that is not found in the responding mammalian host[35]. We propose that the invariant TCR expressed by *i*NKT cells recognizes a previously unknown type of microbe-associated molecular pattern defined by a hexose sugar α-linked to a lipid, usually one with two hydrophobic tails, such as in ceramide or DAG. Furthermore, the abundance of these antigens, and the likely requirement for microbial viability, demonstrate their fundamental importance, similar to that of other microbe-associated molecular patterns.

In summary, we have reported here that the invariant TCR expressed by *i*NKT cells recognized glycolipids from clinically important pathogens with worldwide distributions that cause invasive diseases with high lethality in the absence of antibiotic therapy. The specificity of these responses was conserved in mice and humans, and in mice, the CD1d-presented antigens were required for the activation of $V_\alpha 14i$ NKT cells and host protection. Therefore, we propose that the invariant $V_\alpha$ TCR is a particularly useful one and is evolutionarily conserved, in part because of its ability to recognize a set of widely distributed glycolipids that are an essential part of many microbes, including pathogens.

## METHODS

Methods and any associated references are available in the online version of the paper at http://www.nature.com/natureimmunology/.

**Accession codes.** Protein Data Bank: mouse CD1d-Glc-DAG-s2 structure, 3T1F.

*Note: Supplementary information is available on the Nature Immunology website.*

ACKNOWLEDGMENTS

We thank S. Akira (Osaka University) for *Myd88*$^{-/-}$ mice; B. Beutler (Scripps Research Institute) for *Myd88*$^{-/-}$*Trif*$^{Lps2/Lps2}$ mice; M. Antony (University of Birmingham) for group B *Streptococcus* A909; N. Yamamoto, T. Kinjo, G.D. Ainge, D. Gibson and G. Painter for suggestions; N. Sato for help with glycolipid analysis; and C. Lena for technical assistance. Supported by the US National Institutes of Health (AI45053 and AI71922 to M.K., AI074952 to D.M.Z.; AI070258 to M.T.; and F32AI083029 to J.L.V.), the Japan Society for the Promotion of Science and Ministry of Education, Culture, Sports, Science and Technology (22689031), the Ministry of Health, Labor and Welfare of Japan (H22seisakusouyakuippan012), the Uehara Memorial Foundation (Y.Ki.), the Wellcome Trust, the Royal Society, J. Bardrick (G.S.B.) and the Cancer Research Institute (D.M.Z.).

AUTHOR CONTRIBUTIONS

Y. Kinjo and M.K. designed most the study, except D.M.Z. designed the crystal structure study and the Biacore assay; Y. Kinjo, P.I., J.L.V., E.G., V.N., D.M.Z. and M.K. prepared the manuscript; Y. Kinjo, J.L.V. and B.P. did most of the immunology experiments; P.I., K. Kawahara and A.G.-V. analyzed bacterial glycolipids; P.I., M.I. and C.-H.W. synthesized glycolipids; G.S.B. provided informational support; E.G., Y.L. and D.M.Z. determined the crystal structure of the CD1d-Glc-DAG-s2 complex and did the Biacore assay; X.L., P.R. and M.T. did the human NKT cell experiments; Y. Kinjo, J.L.V., Y. Kaneko, A.O., Y.M. and K. Kawakami did *S. pneumoniae* infection experiments; S.D., S.U. and V.N. prepared bacterial sonicates and provided advice on bacterial culture and infection; A.K. made the mouse CD1d protein; H.Y. and P.W.A. prepared bacteria for glycolipid analysis; and M.K. provided overall supervision.

COMPETING FINANCIAL INTERESTS

The authors declare no competing financial interests.

Published online at http://www.nature.com/natureimmunology/.
Reprints and permissions information is available online at http://www.nature.com/reprints/index.html.

1. Taniguchi, M., Harada, M., Kojo, S., Nakayama, T. & Wakao, H. The regulatory role of Valpha14 NKT cells in innate and acquired immune response. *Annu. Rev. Immunol.* **21**, 483–513 (2003).
2. Brigl, M. & Brenner, M.B. CD1: Antigen presentation and T cell function. *Annu. Rev. Immunol.* **22**, 817–890 (2004).
3. Godfrey, D.I. & Berzins, S.P. Control points in NKT-cell development. *Nat. Rev. Immunol.* **7**, 505–518 (2007).
4. Bendelac, A., Savage, P.B. & Teyton, L. The biology of NKT cells. *Annu. Rev. Immunol.* **25**, 297–336 (2007).
5. Cerundolo, V., Silk, J.D., Masri, S.H. & Salio, M. Harnessing invariant NKT cells in vaccination strategies. *Nat. Rev. Immunol.* **9**, 28–38 (2009).
6. Brossay, L. *et al.* CD1d-mediated recognition of an α-galactosylceramide by natural killer T cells is highly conserved through mammalian evolution. *J. Exp. Med.* **188**, 1521–1528 (1998).
7. Kronenberg, M. & Kinjo, Y. Innate-like recognition of microbes by invariant natural killer T cells. *Curr. Opin. Immunol.* **21**, 391–396 (2009).
8. Nagarajan, N.A. & Kronenberg, M. Invariant NKT cells amplify the innate immune response to lipopolysaccharide. *J. Immunol.* **178**, 2706–2713 (2007).

9. Brigl, M. *et al.* Innate and cytokine-driven signals, rather than microbial antigens, dominate in natural killer T cell activation during microbial infection. *J. Exp. Med.* **208**, 1163–1177 (2011).
10. Kinjo, Y. *et al.* Recognition of bacterial glycosphingolipids by natural killer T cells. *Nature* **434**, 520–525 (2005).
11. Mattner, J. *et al.* Exogenous and endogenous glycolipid antigens activate NKT cells during microbial infections. *Nature* **434**, 525–529 (2005).
12. Kinjo, Y. *et al.* Natural killer T cells recognize diacylglycerol antigens from pathogenic bacteria. *Nat. Immunol.* **7**, 978–986 (2006).
13. Chang, Y.J. *et al.* Influenza infection in suckling mice expands an NKT cell subset that protects against airway hyperreactivity. *J. Clin. Invest.* **121**, 57–69 (2011).
14. O'Brien, K.L. *et al.* Burden of disease caused by *Streptococcus pneumoniae* in children younger than 5 years: global estimates. *Lancet* **374**, 893–902 (2009).
15. Kawakami, K. *et al.* Critical role of Valpha14+ natural killer T cells in the innate phase of host protection against *Streptococcus pneumoniae* infection. *Eur. J. Immunol.* **33**, 3322–3330 (2003).
16. Nakamatsu, M. *et al.* Role of interferon-gamma in $V_{\alpha}14^{+}$ natural killer T cell-mediated host defense against *Streptococcus pneumoniae* infection in murine lungs. *Microbes Infect.* **9**, 364–374 (2007).
17. Brigl, M., Bry, L., Kent, S.C., Gumperz, J.E. & Brenner, M.B. Mechanism of CD1d-restricted natural killer T cell activation during microbial infection. *Nat. Immunol.* **4**, 1230–1237 (2003).
18. Cardell, S. *et al.* CD1-restricted $CD4^{+}$ T cells in major histocompatibility complex class II-deficient mice. *J. Exp. Med.* **182**, 993–1004 (1995).
19. Carapetis, J.R., Steer, A.C., Mulholland, E.K. & Weber, M. The global burden of group A streptococcal diseases. *Lancet Infect. Dis.* **5**, 685–694 (2005).
20. Schrag, S., Gorwitz, R., Fultz-Butts, K. & Schuchat, A. Prevention of perinatal group B streptococcal disease. Revised guidelines from CDC. *MMWR Recomm. Rep.* **51**, 1–22 (2002).
21. Brundish, D.E., Shaw, N. & Baddiley, J. The glycolipids from the non-capsulated strain of Pneumococcus I-192R, A.T.C.C. 12213. *Biochem. J.* **97**, 158–165 (1965).
22. Nakamura, T. *et al.* Serum fatty acid levels, dietary style and coronary heart disease in three neighbouring areas in Japan: the Kumihama study. *Br. J. Nutr.* **89**, 267–272 (2003).
23. Prigozy, T.I. *et al.* Glycolipid antigen processing for presentation by CD1d molecules. *Science* **291**, 664–667 (2001).
24. Kawano, T. *et al.* CD1d-restricted and TCR-mediated activation of valpha14 NKT cells by glycosylceramides. *Science* **278**, 1626–1629 (1997).
25. Li, Y. *et al.* The Valpha14 invariant natural killer T cell TCR forces microbial glycolipids and CD1d into a conserved binding mode. *J. Exp. Med.* **207**, 2383–2393 (2010).
26. Wang, J. *et al.* Lipid binding orientation within CD1d affects recognition of *Borrelia burgorferi* antigens by NKT cells. *Proc. Natl. Acad. Sci. USA* **107**, 1535–1540 (2010).
27. Sidobre, S. *et al.* The T cell antigen receptor expressed by $V_{\alpha}14i$ NKT cells has a unique mode of glycosphingolipid antigen recognition. *Proc. Natl. Acad. Sci. USA* **101**, 12254–12259 (2004).
28. Wun, K.S. *et al.* A molecular basis for the exquisite CD1d-restricted antigen specificity and functional responses of natural killer T cells. *Immunity* **34**, 327–339 (2011).
29. Zajonc, D.M. & Kronenberg, M. CD1 mediated T cell recognition of glycolipids. *Curr. Opin. Struct. Biol.* **17**, 521–529 (2007).
30. Zajonc, D.M. & Wilson, I.A. Architecture of CD1 proteins. *Curr. Top. Microbiol. Immunol.* **314**, 27–50 (2007).
31. Michel, M.L. *et al.* Identification of an IL-17-producing $NK1.1^{neg}$ iNKT cell population involved in airway neutrophilia. *J. Exp. Med.* **204**, 995–1001 (2007).
32. Lu, Y.J. *et al.* Interleukin-17A mediates acquired immunity to pneumococcal colonization. *PLoS Pathog.* **4**, e1000159 (2008).
33. Mallevaey, T. *et al.* A molecular basis for NKT cell recognition of CD1d-self-antigen. *Immunity* **34**, 315–326 (2011).
34. Scott-Browne, J.P. *et al.* Germline-encoded recognition of diverse glycolipids by natural killer T cells. *Nat. Immunol.* **8**, 1105–1113 (2007).
35. Medzhitov, R. & Janeway, C.A. Jr. Innate immunity: the virtues of a nonclonal system of recognition. *Cell* **91**, 295–298 (1997).

## ONLINE METHODS

**Reagents.** Granulocyte-macrophage colony-stimulating factor and α-GalCer were provided by Kyowa Hakko Kirin. *Sphingomonas* GalA-GSL and *B. burgdorferi* BbGL-IIc were synthesized as described[12,36]. Antibodies for staining included anti-CD19 (1D3), anti-CD25 (3C7), anti-CD44 (IM7), anti-CD69 (H1.2F3) and anti-TCRβ (H57-597; all from BD Biosciences); anti-IFN-γ (XMG1.2; BD Biosciences and BioLegend); rat immunoglobulin G1 κ-chain isotype-matched control antibody (R3-34 (BD Biosciences) and RTK2071 (BioLegend)); anti–tumor necrosis factor (MP6-XT22; eBioscience); anti-IL-17a (TC11-18H10.1; BioLegend); and anti-IL-4 (BVD4-1D11; Invitrogen).

**Mice.** C57BL/6 mice and IL-12p35-deficient mice on the C57BL/6 background were from the Jackson Laboratory. *Myd88*$^{-/-}$ mice[37] and *Myd88*$^{-/-}$*Trif*$^{Lps2/Lps2}$ mice[38] on the C57BL/6 background were gifts from S. Akira (Osaka University) and Bruce Beutler (Scripps Research Institute), respectively. All mice were housed under specific pathogen–free conditions and experiments were approved by the Institutional Animal Care and Use Committee of the La Jolla Institute of Allergy & Immunology and the National Institute of Infectious Diseases, Japan.

**Bacterial strains.** For preparation of sonicates for immune assays, bacterial strains *S. pneumoniae* URF918 (clinical isolate, serotype 3)[15], *S. pneumoniae* D39, group B *Streptococcus* COH, group A *Streptococcus* M1, *S. typhimurium* and *E.* coli MC-1061 were used. Bacterial sonicates were generated by the addition of 70% ethanol, followed by washing of the bacteria three times with PBS, then resuspension in PBS at a concentration equivalent to $1 \times 10^9$ colony-forming units per ml before use. For preparation and analysis of glycolipids, bacterial strains *S. pneumoniae* R6 (ref. 39), group B *Streptococcus* A909 (from M. Antony), group B *Streptococcus* (701346; NCIMB), *S. suis* (702644; NCIMB), two group B *Streptococcus* clinical strains belonging to signature types 12 and 17, and *L. casei* (393; American Type Culture Collection) were used. For glycolipid analysis, bacteria were grown at 37 °C in brain-heart–infusion broth (Oxoid) or on agar (Oxoid) supplemented with 5% (vol/vol) defibrinated horse blood. *L. casei* were grown for 16 h at 37 °C in MRS broth (Oxoid).

***S. pneumoniae* infection.** *S. pneumoniae* URF918 cultured in Todd-Hewitt broth (BD) at 37 °C in an incubator at 5% $CO_2$ were collected at a mid-log phase and then washed twice in PBS. For induction of pulmonary infection, mice were anesthetized with isoflurane and restrained on a small board. Mice were inoculated with *S. pneumoniae* ($1 \times 10^6$ to $1 \times 10^7$ colony-forming units in a volume of 50 μl per mouse) by insertion of a 24-gauge catheter into the trachea. For induction of systemic infection, *S. pneumoniae* ($1 \times 10^7$ colony-forming units) were injected intravenously into mice. For blockade of CD1d, mice were treated intraperitoneally with 200 μg anti-CD1d (1B1; BD Biosciences and eBioscience) or rat immunoglobulin G2b isotype-matched control antibody (EB149; 10H5; eBioscience) 6–24 h before and just before infection. At 6 h (spleen) or 13 h (lung), lung mononuclear cells or spleen cells were collected as reported[15,40], and CD19$^-$ cells positive for the α-GalCer-loaded CD1d tetramer were analyzed immediately after isolation for intracellular cytokines without restimulation or pretreatment with brefeldin. For measurement of the lung bacterial burden, tissues were collected at day 3 after infection and were homogenized in PBS by being 'teased' with a stainless steel mesh. Homogenates were inoculated in a volume of 100 μl on 5% (vol/vol) sheep blood Mueller-Hinton agar plates and cultured for 18 h, followed by colony counting. For isolation of CD11c$^+$ cells, spleens were collected at 16–18 h after infection with *S. pneumoniae* or injection of GalA-GSL (20 μg) or α-GalCer (1 μg), and CD11$^+$ cells were purified from spleen cells with an EasySep Mouse CD11c Positive Selection Kit according to the company's instructions (StemCell Technologies). CD11c$^+$ cells ($1 \times 10^5$) were cultured for 16–18 h with CD1d-reactive hybridomas ($5 \times 10^4$ cells), and IL-2 in supernatants was measured by enzyme-linked immunosorbent assay (BD Bioscience).

**Lipid extraction and purification from bacteria.** For lipid purification, bacteria were grown to late exponential phase and were collected by centrifugation at 1,800*g* for 15 min. Lipids were extracted from washed cells and purified as described[41]. Lipid extracts were assessed by thin-layer chromatography on aluminum-backed plates of silica gel 60 $F_{254}$ (5554; Merck), with $CHCl_3$, $CH_3OH$ and $H_2O$ (65:25:4 (vol/vol/vol)). Glycolipids were visualized by spraying of the plates with α-naphthol–sulfuric acid, followed by gentle charring of plates. Other types of lipids were visualized by spraying of the plates with 5% (vol/vol) ethanolic molybdophosphoric acid followed by charring, or by spraying of the plates with a Dittmer and Lester reagent specific for phospholipids. *L. casei* lipids were fractionated on a column of DEAE-cellulose. The chloroform-methanol fraction (2:1 (vol/vol)) was collected and concentrated.

**Cell-free antigen-presentation assay.** CD1d-reactive hybridomas have been described[10,12]. T cell hybridomas on CD1d-coated plates were stimulated according to published protocols[10,12,40]. Bacterial sonicates or compounds were incubated for 24 h in microwells coated with 1.0 μg mouse CD1d. After being washed, $5 \times 10^4$ to $1 \times 10^5$ $V_\alpha 14i$ NKT cell hybridoma cells or control cells were cultured in the plates for 16–20 h, and IL-2 in the supernatant was measured by enzyme-linked immunosorbent assay (BD Pharmingen).

***In vivo* responses to microbial glycolipids and flow cytometry.** Activation-marker expression and intracellular cytokine production by cells positive for the α-GalCer–CD1d tetramer were analyzed according to published protocols[10]. Mouse DCs were prepared by culture of bone marrow progenitor cells for 7 d with mouse granulocyte-macrophage colony-stimulating factor. Mouse DCs were incubated for 24 h with *S. pneumoniae* glycolipids (20 μg/ml), group B *Streptococcus* glycolipids (20 μg/ml), GalA-GSL (10 μg/ml) or α-GalCer (0.1 μg/ml). After being washed with PBS, glycolipid-pulsed DCs ($5 \times 10^5$) were injected intravenously into mice. Liver mononuclear cells positive for the α-GalCer–CD1d tetramer were analyzed (without further treatment) 4 h or 14 h later for activation markers and intracellular cytokines. Cells were analyzed with a FACSCalibur or LSR II (BD Bioscience) and FlowJo software.

**$V_\alpha 24i$ NKT cell response.** Human $V_\alpha 24i$ NKT cell lines were generated with modifications to a published protocol[10]. $V_\alpha 24i^+$ T cells were isolated from LeukoPak cells with magnetic beads (Miltenyi Biotec) coupled to mAb to $V_\alpha 24$ (6B11; eBioscience), and were cultured for 10 d with irradiated autologous immature DCs (3,000 rads) in the presence of α-GalCer (100 ng/ml) and human recombinant IL-2 (10 IU/ml; R&D Systems). After a second stimulation with α-GalCer-pulsed irradiated autologous immature DCs, cell lines were 95% $V_\alpha 24^+$. $V_\alpha 24i$ NKT cells ($3 \times 10^4$) were cultured with $3 \times 10^4$ irradiated HeLa cells ($3 \times 10^4$; 10,000 rads) transfected to express human CD1d, in the presence of glycolipids. IFN-γ or IL-4 in supernatants was measured by enzyme-linked immunosorbent assay (eBioscience) after 24 h.

**Additional methods.** Information on nuclear magnetic resonance analysis, fatty acid analysis, double-bond localization, mass spectrometric analysis, and mouse CD1d-Glc-DAG-s2 crystallization and structure determination is available in the **Supplementary Results**, **Supplementary Methods** and **Supplementary References.**


36. Wu, D. *et al.* Bacterial glycolipids and analogs as antigens for CD1d-restricted NKT cells. *Proc. Natl. Acad. Sci. USA* **102**, 1351–1356 (2005).
37. Adachi, O. *et al.* Targeted disruption of the MyD88 gene results in loss of IL-1- and IL-18-mediated function. *Immunity* **9**, 143–150 (1998).
38. Hoebe, K. *et al.* Identification of Lps2 as a key transducer of MyD88-independent TIR signalling. *Nature* **424**, 743–748 (2003).
39. Pearce, B.J., Iannelli, F. & Pozzi, G. Construction of new unencapsulated (rough) strains of *Streptococcus pneumoniae*. *Res. Microbiol.* **153**, 243–247 (2002).
40. Tupin, E. & Kronenberg, M. Activation of natural killer T cells by glycolipids. *Methods Enzymol.* **417**, 185–201 (2006).
41. Fischer, W. The polar lipids of group B Streptococci. I. Glucosylated diphosphatidylglycerol, a novel glycopholipid. *Biochim. Biophys. Acta.* **487**, 74–88 (1977).




doi:10.1038/ni.2096

# Unique Interplay between Sugar and Lipid in Determining the Antigenic Potency of Bacterial Antigens for NKT Cells

**Enrico Girardi[1☯], Esther Dawen Yu[1☯], Yali Li[1], Norihito Tarumoto[2,3], Bo Pei[4], Jing Wang[1], Petr Illarionov[5], Yuki Kinjo[2], Mitchell Kronenberg[4], Dirk M. Zajonc[1]***

**1** Division of Cell Biology, La Jolla Institute for Allergy & Immunology, La Jolla, California, United States of America, **2** Department of Chemotherapy and Mycoses, National Institute of Infectious Diseases, Tokyo, Japan, **3** Department of Infectious Disease and Infection Control, Saitama Medical University, Saitama, Japan, **4** Division of Developmental Immunology, La Jolla Institute for Allergy & Immunology, La Jolla, California, United States of America, **5** School of Biosciences, University of Birmingham, Edgbaston, Birmingham, United Kingdom

## Abstract

Invariant natural killer T (iNKT) cells are an evolutionary conserved T cell population characterized by features of both the innate and adaptive immune response. Studies have shown that iNKT cells are required for protective responses to Gram-positive pathogens such as *Streptococcus pneumoniae*, and that these cells recognize bacterial diacylglycerol antigens presented by CD1d, a non-classical antigen-presenting molecule. The combination of a lipid backbone containing an unusual fatty acid, vaccenic acid, as well as a glucose sugar that is weaker or not stimulatory when linked to other lipids, is required for iNKT cell stimulation by these antigens. Here we have carried out structural and biophysical studies that illuminate the reasons for the stringent requirement for this unique combination. The data indicate that vaccenic acid bound to the CD1d groove orients the protruding glucose sugar for TCR recognition, and it allows for an additional hydrogen bond of the glucose with CD1d when in complex with the TCR. Furthermore, TCR binding causes an induced fit in both the sugar and CD1d, and we have identified the CD1d amino acids important for iNKT TCR recognition and the stability of the ternary complex. The studies show also how hydrogen bonds formed by the glucose sugar can account for the distinct binding kinetics of the TCR for this CD1d-glycolipid complex. Therefore, our studies illuminate the mechanism of glycolipid recognition for antigens from important pathogens.

**Citation:** Girardi E, Yu ED, Li Y, Tarumoto N, Pei B, et al. (2011) Unique Interplay between Sugar and Lipid in Determining the Antigenic Potency of Bacterial Antigens for NKT Cells. PLoS Biol 9(11): e1001189. doi:10.1371/journal.pbio.1001189

**Academic Editor:** Philippa Marrack, National Jewish Medical and Research Center/Howard Hughes Medical Institute, United States of America

**Received** February 2, 2011; **Accepted** September 20, 2011; **Published** November 1, 2011



**Funding:** This work was funded by US NIH grants RO1 AI074952 (DMZ), RO1 AI45053, and R37 AI71922 (MK); grants from the Ministry of Education, Culture, Sports, Science and Technology of Japan and JSPS (22689031); and from the Ministry of Health, Labor and Welfare of Japan (H22seisakusouyakuippan012)(YK). DMZ is recipient of an investigator award from the Cancer Research Institute. The authors have no conflicting financial interests. The funding agencies had no role in study design, data collection and analysis, decision to publish, or preparation of the manuscript.

**Competing Interests:** The authors have declared that no competing interests exist.

**Abbreviations:** α-GalCer, α-galactosylceramide; BbGL-2c, *Borrelia burgorferi* glycolipid 2c; β2m, beta-2-microglobulin; CDR, complementarity determining regions; DAG, diacylglycerol; GalAGSL, galacturonosyl-glycosphingolipid from *Sphingomonas* spp.; Glc-DAG-s2, glucose diacylglycerol lipid from *Streptococcus pneumoniae* with a vaccenic acid in position *sn*-2; iNKT, invariant Natural Killer T; $k_a$, association rate constant; $k_d$, dissociation rate constant; $K_D$, equilibrium dissociation constant; mCD1d, mouse CD1d

* E-mail: dzajonc@liai.org

☯ These authors contributed equally to this work.

## Introduction

Invariant NKT cells (iNKT) are an evolutionarily conserved population of T lymphocytes able to respond to lipid antigens when presented by CD1d, a non-classical MHC class I–like molecule [1].

Antigen recognition by iNKT cells is mediated by a semi-invariant αβ T cell receptor (TCR) formed by a conserved Vα14-Jα18 rearrangement (Vα24-Vα18 in humans), and a limited panel of pairing β chains (Vβ8.2, Vβ7, Vβ2 in mouse; Vβ11 in humans). The number of antigens recognized by these cells has increased in the last few years, following the discovery of α-galactosylceramide (α-GalCer), the prototypical iNKT antigen [2]. Although the nature of the predominant self-antigens recognized by iNKT cells still remains controversial, important progress has been made in describing the microbial antigens recognized by this cell type. Glycosphingolipids from *Sphingomonas* spp. and diacylglycerol (DAG) ligands from *Borrelia burgdorferi*, the causative agent of Lyme disease, were identified to stimulate iNKT cells in a CD1d/TCR-dependent manner [3–7]. As *Sphingomonas* spp. and *B. burgdorferi* are not responsible for widespread or lethal diseases, we considered it possible that more pathogenic organisms also express iNKT antigens, which would account for the highly conserved nature of the CD1d-iNKT TCR interaction. Indeed, recent studies identified the structures of DAG compounds from the highly pathogenic *Streptococcus pneumoniae* (*S. pneumoniae*) and *Group B streptococcus* (GBS), which were able to stimulate iNKT cells [8]. In vitro and in vivo assays demonstrated surprisingly strict requirements for these antigens in activating iNKT cells. The most potent *S. pneumoniae* antigen, Glc-DAG-s2, is characterized by having a *sn*-

## Author Summary

Invariant natural killer T (iNKT) cells are an evolutionarily conserved population of immune cells that recognize lipid antigens. A protein called a T cell receptor for antigen (TCR) on the surface of these iNKT cells recognizes lipids bound to a protein called CD1d on the surface of antigen-presenting cells. Here we describe the three-dimensional structure of the complex that forms between CD1d and the iNKT TCR together with a glycolipid antigen from the infectious bacterium *Streptococcus pneumoniae*, which is a common cause of bacterial meningitis in adults and is responsible for many other pneumococcal infections. We determined the three-dimensional structure of the complex by X-ray crystallography. The data obtained allow us to understand the structural requirements that make this glycolipid a potent antigen for iNKT cells, and why the TCR of these cells recognizes a particular combination of hexose sugar and diacylglycerol lipid. Moreover, by mutating CD1d and using biophysical methods to study the mutant protein complexes, we analyzed the role of the protein–protein interface between CD1d and the TCR and found that it plays an important role in the stability, but not the formation, of the trimolecular complex containing glycolipid antigen.


3 linked glucose, a *sn*-1 linked palmitic acid (C16:0), and most importantly, the presence of *cis*-vaccenic acid (C18:1, n-7) in position *sn*-2 of the glycerol moiety. This uncommon fatty acid was required for significant activity, since the positional isomer with a vaccenic acid in position *sn*-1 failed to elicit a strong activation, as did the homologous compounds containing an oleic acid (C18:1, n-9). Moreover, the same antigen showed the ability to stimulate both mouse and human iNKT cells, unlike the previously characterized DAG antigens from *B. burgdorferi* [6]. Interestingly, previous studies showed that glucose-containing glycolipids are relatively weaker antigens compared to the one containing galactose or galacturonic acid [2,3,9,10], while the glucose isomer of the *B. burgdorferi* glycolipid 2c (BbGL-2c) is not antigenic at all [6]. It is therefore surprising that the glucose-containing *S. pneumoniae* Glc-DAG-s2 is such a potent antigen in eliciting iNKT cell responses.

In order to determine the molecular basis for the stringent structural requirements for recognition of the *S. pneumoniae* antigen Glc-DAG-s2, and to further analyze the mechanism of the mouse CD1d (mCD1d)-iNKT TCR complex formation, we determined the structure of the mCD1d-Glc-DAG-s2-iNKT TCR complex by X-ray crystallography and we analyzed the role of the F′ roof in the formation and stability of mCD1d-iNKT TCR complexes. Our data show how the combination of *cis*-vaccenic acid and glucose is required for the formation of novel protein-antigen contacts, resulting in the relatively strong affinity of this ligand for the iNKT TCR.

## Results

### mCD1d-Glc-DAG-s2-TCR Structure

Previous biophysical analysis of the kinetics of interaction of the mCD1d-Glc-DAG-s2 complex with the iNKT TCR revealed a TCR interaction with a low micromolar affinity [8]. Overall, Glc-DAG-s2 complexes with mouse CD1d are characterized by a comparable but slightly higher affinity for the iNKT TCR compared to those containing the other known bacterial DAG antigen BbGL-2c ($K_D$ of 4.4 and 6.2 μM, respectively), consistent with the similar antigenic potencies of these compounds [8,11]. However, complexes containing Glc-DAG-s2 have significantly different binding kinetics compared to those containing BbGL-2c, with Glc-DAG-s2 showing considerably slower association and dissociation rates. In order to investigate the molecular basis for this different kinetic behavior and the role of the unique structural features of this ligand in determining its antigenicity, we determined the crystal structure of the mCD1d-Glc-DAG-s2-iNKT TCR complex at 2.7 Å resolution (Figure 1, Table 1).

The structure shows the conserved "parallel" docking mode of the iNKT TCR on the CD1d-ligand complex (Figure1A) [12–14]. As a consequence of this unique binding mode, the TCR α chain mediates the majority of the contacts with the CD1d-Glc-DAG-s2 complex, with additional contacts with CD1d provided by the CDR2β, CDR3β, and, to a lesser extent, the CDR1β loops (Table S1). Well-defined, unbiased density was present for the ligand, superior to what has been observed for the mCD1d-Glc-DAG-s2 complex in absence of the TCR [8], suggesting that the ligand adopts a more rigid and ordered conformation upon TCR binding (Figure 1B, Figure S1). Similar to the antigens previously characterized, the TCR CDR1α and CDR3α loops exclusively mediate contacts between the TCR and the antigen (Figure 2A). In particular, the TCR recognizes the 2′-OH and 3′-OH positions of the hexose ring via H bonds with Gly96 and Asn30 on the α chain, highlighting the importance of these two hydroxyl groups on the antigen in the formation of the complex. However, due to the presence of a glucose on Glc-DAG-s2, the 4′ hydroxyl group is no longer able to interact with Asn30 on the α chain, in contrast to other galactose-containing glycolipids. Previous studies showed that the contacts between the ligand and the iNKT dominate the initial association phase of the interaction [9]. The loss of an H bond at the ligand-TCR interface, although not sufficient to

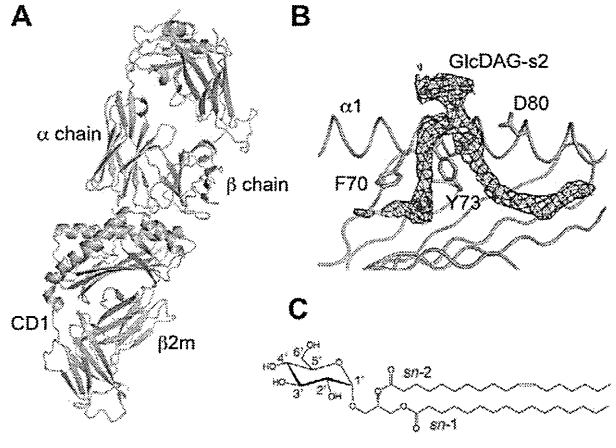


**Figure 1. Structure of the mCD1d-Glc-DAG-s2-TCR complex.** (A) Cartoon representation of the mCD1d-Glc-DAG-s2-TCR trimolecular complex with the CD1d/β2m protein in grey, and the TCR α and β chains in cyan and orange, respectively. The Glc-DAG-s2 antigen is shown as yellow sticks, tucked at the interface between CD1d and the TCR. (B) Side-view of the antigen-binding groove in the mCD1d-Glc-DAG-s2-TCR complex with the DAG antigen shown in sticks and the α2 helix removed for clarity. The 2Fo−Fc electron density map is contoured at 1σ and shown as a blue mesh around the glycolipid ligand. Several mCD1d residues interacting with the lipid are depicted. (C) Chemical structure of the Glc-DAG-s2 antigen with vaccenic acid in the *sn*-2 position.
doi:10.1371/journal.pbio.1001189.g001

**Table 1.** Data collection and refinement.

| Statistics | mCD1d-Glc-DAG-s2-TCR |
|---|---|
| **Data collection** | |
| Space group | $C222_1$ |
| Cell dimension | |
| *a*, *b*, *c*, (Å) | 78.1, 190.7, 150.9 |
| α, β, γ (°) | 90.0, 90.0, 90.0 |
| Resolution range (Å) [outer shell] | 44.5–2.70 [2.85–2.70] |
| No. reflections | 31,376 |
| $R_{merge}$ (%) | 13.5 [53.0] |
| $R_{pim}$ (%) | 7.5 [30.0] |
| $R_{meas}$ (%) | 15.5 [61.2] |
| Multiplicity | 4.0 [4.0] |
| Average I/σI | 7.1 [2.4] |
| Completeness (%) | 99.8 [99.9] |
| **Refinement statistics** | |
| No. atoms | 6,554 |
| Protein | 6,276 |
| Ligand | 53 |
| Carbohydrate | 80 |
| Waters | 145 |
| $R/R_{free}$ | 0.203/0.257 |
| Ramachandran plot (%) | |
| Favored | 97.1 |
| Allowed | 100.0 |
| R.m.s. deviations | |
| Bonds (Å) | 0.010 |
| Angles (°) | 1.275 |
| B-factors (Å$^2$) | |
| Protein | 37.4 |
| Ligand | 44.6 |
| Carbohydrate | 57.3 |
| Waters | 30.4 |

doi:10.1371/journal.pbio.1001189.t001

abolish the binding of the iNKT TCR to the mCD1d-Glc-DAG-s2 complex, is therefore likely to decrease the association rate.

## Induced Fit of the Glycolipid upon TCR Binding

When the structures of the mCD1d-Glc-DAG-s2 complex in the presence or absence of the TCR are compared, important conformational changes are observed for the ligand (Figure 2B). Consistent with what was observed for the mCD1d-Glc-DAG-s2 structure in the absence of the TCR [8], the *sn*-2 vaccenic acid is bound in the A′ pocket while the *sn*-1 palmitic acid occupies the F′ pocket. However, while in the absence of the TCR the vaccenic acid encircles the A′ pole in a clockwise manner, the opposite orientation is preferred in the ternary complex, although residual density also suggests some equilibrium between the two orientations. Moreover, upon TCR ligation, the glucose moiety is shifted by about 30 degrees clockwise around its glycosidic bond to assume a position at the center of the binding groove as observed for other TCR-bound glycolipid antigens (Figure 2B). Similar to what has been described for BbGL-2c, this conformational change requires the breaking of several contacts with CD1d and the formation of new hydrogen bonds with the α2 helix of CD1d and the TCR α chain. In particular, a hydrogen bond with Arg79 on the α1 helix is lost while new polar contacts are formed with Asp153 and Thr156 on the α2 helix upon TCR binding, resulting in a final orientation conserved among α-linked sugars [13–15]. As proposed for BbGL-2c, these conformational changes likely contribute to the slower association rate of the TCR when binding DAG microbial antigen-mCD1d complexes compared to sphingolipid-containing antigens [14]. However, the presence of glucose on Glc-DAG-s2 results in an additional H bond between the antigen and the backbone of the α2 helix of CD1d, involving the carbonyl group of glycine 155 (3.2 Å, Figure 2B). Because this contact stabilizes a favorable binding conformation of the antigen in the binding groove, it is likely that this feature is contributing to the slower complex dissociation observed for this ligand compared to BbGL-2c, as the TCR has to invest less energy to lock the glucose into place. Moreover, comparison of the mCD1d-TCR molecular contacts in the two DAG antigens ternary complexes revealed a slightly optimized interface for Glc-DAG-s2 compared to BbGL-2c (involving in particular additional salt bridges between CDR3α and CDR2β residues with mCD1d; Table S1; [14]), which could have a further stabilizing effect on the dissociation rate of the ternary complex.

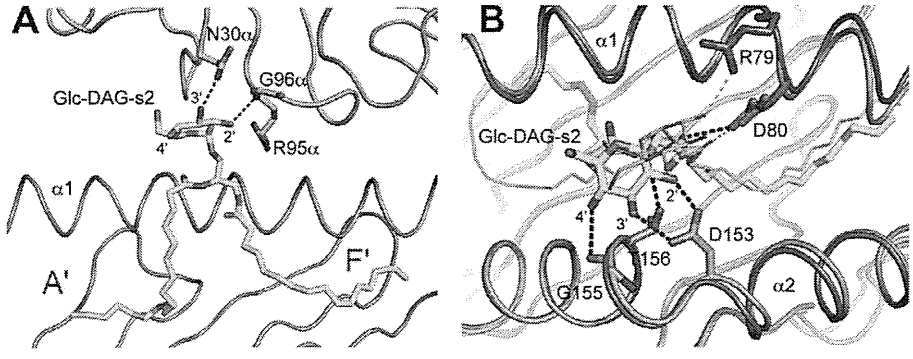


**Figure 2. Binding of Glc-DAG-s2 to mCD1d and the TCR.** (A) Contacts between Glc-DAG-s2 and the iNKT TCR. The conserved hydrogen bonds, involving key residues on CDR1α and CDR3α of the TCR, are shown as dashed blue lines. Glc-DAG-s2, yellow; mCD1d heavy chain, grey; TCR α chain, cyan; TCR β chain, orange. Top (B) view of the mCD1d interactions with Glc-DAG-s2 in the presence (grey, Glc-DAG-s2 in yellow) or absence (dark grey, Glc-DAG-s2 in cyan) of the TCR. Hydrogen bond interactions between mCD1d residues and the polar moieties of Glc-DAG-s2 are indicated with blue dashed lines for the ternary complex and cyan for the mCD1d-Glc-DAG-s2 complex.
doi:10.1371/journal.pbio.1001189.g002

## Interplay between the Sugar and Lipid for Determining Antigenicity

When the structures of the ternary complexes of the DAG antigens Glc-DAG-s2 and BbGL-2c are compared (Figure 3), it is interesting to note how the unsaturations present on the respective vaccenic and oleic acids are localized in the same portion of the mCD1d A′ pocket, suggesting a preference for this region of the groove for binding unsaturated alkyl chains. Consistent with this, it was previously noted that the presence of unsaturations improved the stability of the mCD1d-glycolipid complex, possibly due to the kink introduced in the alkyl chain by the unsaturated bonds, which could nicely sit at the bottom of the channel connecting the A′ pocket with the protein surface [16,17]. Assuming that an unsaturated fatty acid would preferentially bind in the A′ pocket, in the positional isomer of Glc-DAG-s2 having the vaccenic acid at the *sn*-1 position, this would result in a reversed orientation of the glycerol backbone in the binding groove. The reversed glycerol orientation would cause an unfavorable positioning of the glucose head, therefore explaining the lack of antigenic activity for this compound [8].

A superposition of the mCD1d-Glc-DAG-s2 and mCD1d-BbGL-2c complexes in presence of the TCR shows how the two hexose groups are oriented slightly differently at the opening of the binding groove (Figure 3A). The lack of activity of the Glc-DAG-s2 analog containing an oleic acid in place of vaccenic acid suggests that the vaccenic acid is required for a more favorable orientation of the exposed glucose, possibly enhancing the ability of the glucose moiety to contact Gly155 and therefore positioning it in a more stable fashion in the correct orientation for TCR recognition. Galactose and glucose differ only with regard to the orientation of the 4′ hydroxyl on the hexose sugar ring, with the axial orientation for galactose and the equatorial orientation, i.e., closer to the plane of the ring, for glucose. Despite the structural similarity of the two sugars, intriguingly, the galactose-containing version of the *S. pneumoniae* DAG glycolipid antigen with a *sn*-2 vaccenic acid, called Gal-DAG-s2, was not able to activate mouse iNKT cell hybridomas (Figure 4). A drastically reduced response was also observed for the Gal-DAG-s1 ligand. This indicates that the presence of vaccenic acid in the A′ pocket of the mCD1d binding groove does not automatically confer antigenicity. When the stereochemistry of the 4′ carbon is inverted, converting the glucose of Glc-DAG-s2 into galactose, it becomes clear that the 4′-OH group will be too distant (4.3 Å, Figure S2) to engage Asn30 on the CDR3α loop, while at the same time losing the contact with Gly155 on the α2 helix of mCD1d. Even if a further reorientation of the galactose sugar by the iNKT TCR were possible, this would require an additional energetic toll, suggesting a rationale for the reduced activity of the Gal-DAG-s2 compound. It is therefore evident that the combination of the uncommon vaccenic acid and the glucose sugar, which is relatively weak in the context of other DAG antigens and glycosphingolipids, is required for the optimal positioning of the Glc-DAG-s2 antigen in the mCD1d binding groove for TCR recognition.

## The mCD1d F′ Roof Affects Recognition by the iNKT TCR

The structures of the iNKT cell TCR in complex with different mCD1d-microbial antigens complexes showed how the iNKT TCR is able to induce conformational changes in both the ligand and mCD1d upon complex formation [14]. In particular, the insertion of amino acid Leu99α, located on the CDR3α loop of the iNKT TCR, between residues Leu84, Val149, and Leu150 above the F′ pocket of mCD1d, resulted in several new van der Waals (VdW) contacts and the formation of a hydrophobic surface above the pocket (F′ roof). Consistent with this, a comparison of mCD1d-Glc-DAG-s2 structures before and after TCR binding reveals that the F′ roof also is formed for this antigen upon TCR binding (Figure 5A).

In order to understand and validate the role of the F′ roof in the formation of a more stable CD1d-Glc-DAG-s2-TCR complex, we mutated selected residues involved in the formation of the roof and characterized the ability of the mutated mCD1d proteins to stimulate iNKT cell hybridomas. As a complete removal of the F′ roof would likely result in an abrogation of binding, as demonstrated by the loss of function mutation of L99α in the TCR to alanine [18], we chose mutations of the relevant position in mCD1d that would maintain the hydrophobic nature of their side chains, in order to perturb the F′ roof area without making a too drastic change. We therefore used site-directed mutagenesis to generate the following mCD1d substitutions: Leu84Val, Leu84Phe, the latter mimicking the human homolog, Val149Leu and Leu150Val, together with two control mutants, Met69Ala and Met162Ala from the area above the A′ pocket (Figure 5A). Interestingly, we obtained drastically reduced expression yields for the Leu84Val mutant, and this construct was not tested further. The iNKT cell hybridomas Hy2C12 (bearing the Vα14Vβ8.2 TCR used in our structural studies), Hy1.2 (also Vα14Vβ8.2), and Hy1.4 (expressing a less common Vα14Vβ10 TCR) were tested for their ability to respond to mCD1d-glycolipid complexes in an

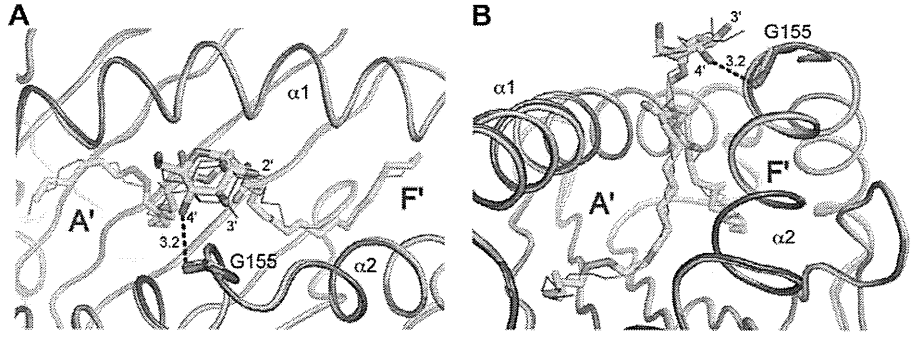


**Figure 3. Binding of Glc-DAG-s2 and BbGL-2c to mCD1d.** Top (A) and side (B) view of the mCD1d interactions in the presence of the TCR. Glc-DAG-s2 is shown in yellow and BbGL-2c in blue and thin lines with the respective CD1d structure in grey and blue. The novel hydrogen bond formed between G155 on the α2 helix and the 4′-OH of Glc-DAG-s2 is indicated with a blue dashed line with its distance expressed in Å. The unsaturations in the alkyl chains are shown in green and sit in a similar region of the A′ pocket.
doi:10.1371/journal.pbio.1001189.g003

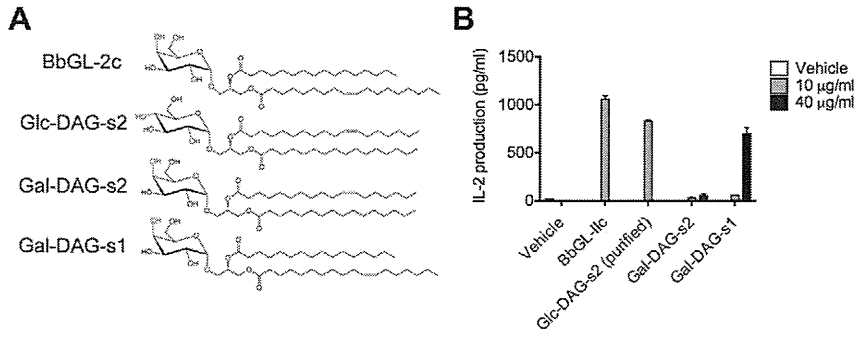


**Figure 4. Stringent specificity requirements for recognition of the *S. pneumoniae* iNKT antigens.** (A) Chemical structure of bacterial antigens BbGL-2c and Glc-DAG-s2 together with galactose-containing versions of Glc-DAG-s2. The 4′ hydroxyl group, which differs in orientation between glucose and galactose and the unsaturations of the antigens, is shown in red. (B) Antigen presenting cells expressing mCD1d were pulsed with the indicated amounts of each compound and were then cultured with iNKT cell hybridoma 1.2. IL-2 amounts in the culture supernatant are shown. The error bars indicate the SEM of triplicate measurements and the data are representative of four separate experiments. Due to their relatively strong response, BbGL-2c and Glc-DAG-s2 were tested exclusively at 10 μg/ml.
doi:10.1371/journal.pbio.1001189.g004

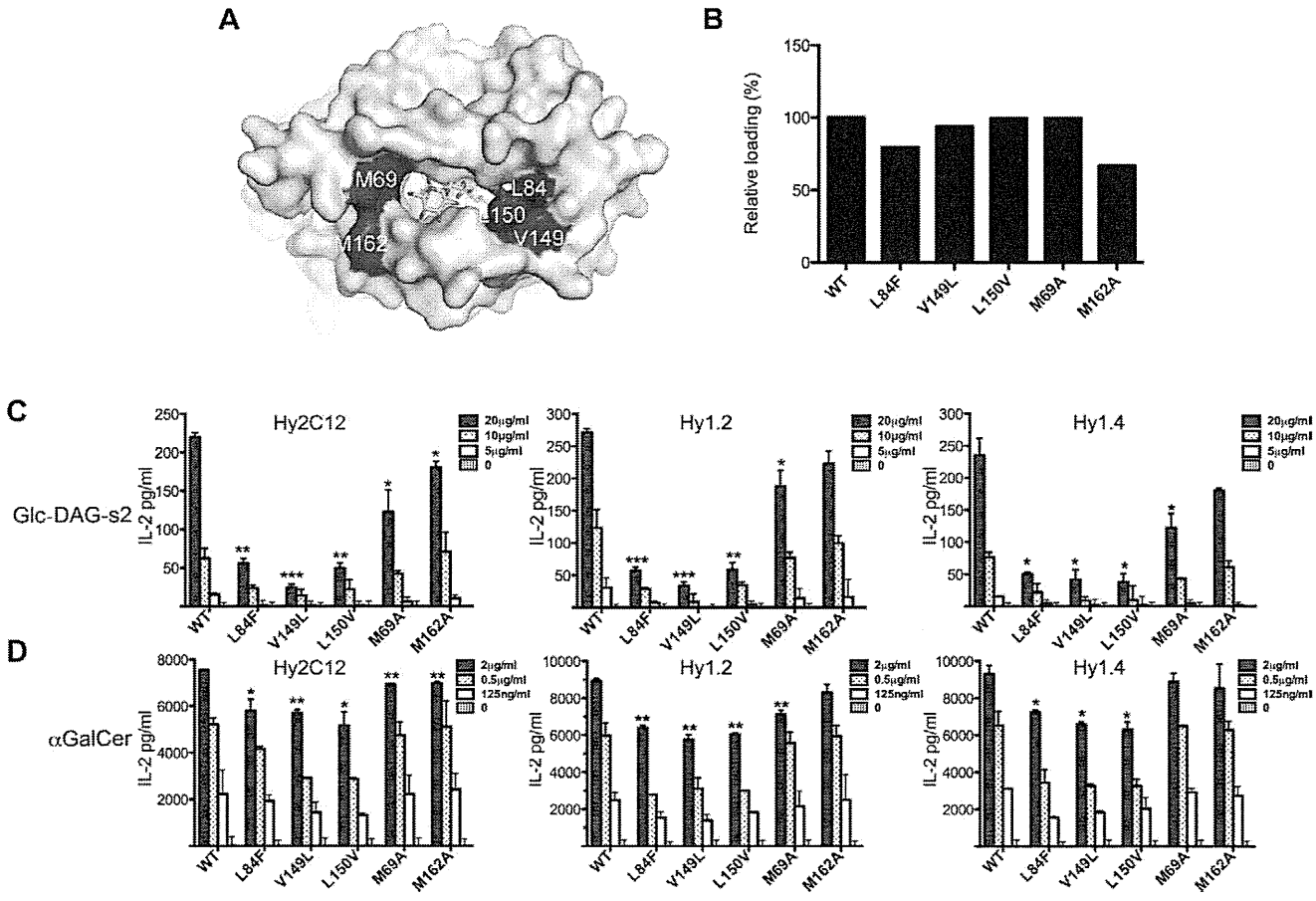


**Figure 5. Antigen presentation by F′ roof mutants.** (A) Surface of the mCD1d-Glc-DAG-s2 structure in the presence (grey, Glc-DAG-s2 in yellow) of the iNKT TCR. The residues mutated for further analysis are shown in blue. (B) Relative antigen loading efficiencies by the mCD1d mutants as determined by surface plasmon resonance. Values are expressed as percentages with the WT protein set at 100%. The ability of CD1d mutants to present Glc-DAG-s2 (C) and α-GalCer (D) was analyzed in a cell free antigen presentation assay using CD1d coated plates and the Vα14*i* NKT cell hybridomas Hy2C12, Hy1.2, Hy1.4. As a measure of direct iNKT cell activation IL-2 was measured in the culture supernatant by ELISA. Each bar shows mean + SD from duplicate wells and is representative of two independent experiments.
doi:10.1371/journal.pbio.1001189.g005

antigen presenting cell-free assay using mCD1d-coated plates. IL-2 secretion provided a measure of TCR stimulation. We stimulated the cells with either Glc-DAG-s2 or α-GalCer, the prototypical iNKT cell antigen that induces a preformed F′ roof on mCD1d [19]. When loaded with Glc-DAG-s2 or α-GalCer, all the mutants showed a reduced ability to stimulate the hybridoma (Figure 5). In particular, the mutants Leu84Phe and Val149Leu abrogated iNKT cell activation, while a slightly reduced activity was observed with the Leu150Val mutant.

As the reduced response could be the consequence of impaired loading of these antigens on mCD1d, we measured the loading efficiency of α-GalCer on each mutant by surface plasmon resonance (SPR) using a monoclonal antibody (L363 [20]) specifically reactive to complexes of mCD1d with α-GalCer and analogs (Figure 5B). Although the Leu84Phe and Met62Ala mutants showed lower levels of antigen loading compared to wild type mCD1d, loading on the mutated mCD1d proteins was never below 65% of the wild type control, and does not appear to correlate directly with the ability of the mutated proteins to stimulate the iNKT cell hybridoma. Although the lack of an antibody able to recognize the mCD1d-Glc-DAG-s2 complex did not allow us to assess the loading of this antigen onto the mCD1d mutants, we believe it is unlikely that the two ligands have radically different loading efficiencies, suggesting a critical role of the area above the F′ pocket in the TCR interaction with mCD1d/Glc-DAG-s2 and mCD1d/α-GalCer.

## Mutation of F′ Roof Residues Affects Preferentially the Stability of the mCD1d-iNKT TCR Complex

We previously hypothesized that the formation of the F′ roof on CD1d affects the stability of the CD1d interaction with the iNKT TCR [14]. To validate this hypothesis we measured the effect of the F′ roof mutants on the binding kinetics of the mCD1d-iNKT TCR complex (Figure 6). Because of the relatively weak antigenicity of Glc-DAG-s2 compared to α-GalCer, the latter was chosen for SPR analysis. A comparison of the affinities shows how all the F′ roof mutants have weaker affinities for the iNKT TCR, Leu84Phe being the weakest with a ~4-fold reduction compared to the wild type protein (Figure 6) while the two control mutants showed affinities and kinetics similar to the wild type protein. Strikingly, the differences in affinities between mCD1d F′ roof variants derive mainly from faster dissociation rates for the mutant complexes, while the association rates are minimally affected by perturbation of the F′ roof. Mutation of residues Val149 and L150 appear less disruptive than mutation of Leu84, as the Leu84Phe has the fastest dissociation rate. Taken together, these data suggest that the F′ roof is critical in determining the dissociation rate and therefore the stability of the mCD1d-TCR complex.

## Discussion

Activation of iNKT cells can result as a consequence of TCR-independent, IL12-dependent signals and/or through the recognition of self and foreign antigens by its semi-invariant TCR, with the latter mechanism playing an important role in modulating the overall response [21]. The recent discovery that highly pathogenic Gram-positive bacteria express antigens recognized by both mouse and human iNKT cells [8] therefore opens important perspectives for the development of therapeutic agents against pneumonia and meningitis, while also suggesting a potential rationale for the conserved features of the CD1d-TCR interaction among different mammalian species.

A

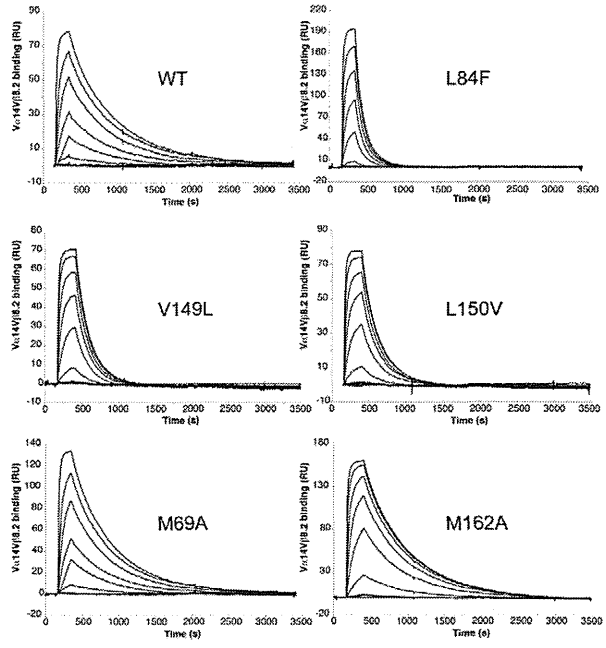


B

| | $K_d$ (nM) | $k_a$ ($x10^4$ $M^{-1}$ $s^{-1}$) | $k_d$ ($x10^{-3}$ $s^{-1}$) |
|---|---|---|---|
| WT | 39.9 ± 5.4 | 4.17 ± 0.89 | 1.65 ± 0.14 |
| L84F | 177.5 ± 21.9 | 5.67 ± 2.20 | 9.83 ± 2.66 |
| V149L | 102.0 ± 1.4 | 6.11 ± 1.07 | 6.24 ± 1.03 |
| L150V | 83.4 ± 5.4 | 6.10 ± 1.92 | 5.11 ± 1.18 |
| M69A | 44.2 ± 5.9 | 5.35 ± 2.33 | 2.30 ± 0.74 |
| M162A | 39.5 ± 3.2 | 5.32 ± 1.41 | 2.08 ± 0.39 |

**Figure 6. F′ roof mutations affect the stability of the mCD1d-iNKT cell TCR complex.** (A) Binding response of a Vα14Vβ8.2 TCR to immobilized mouse CD1d loaded with α-GalCer as measured by surface plasmon resonance. Binding of increasing concentrations of the TCR is shown for each mutant as black lines. (B) Kinetic parameters measured for WT and mutants proteins.
doi:10.1371/journal.pbio.1001189.g006

Surprisingly, the *S. pneumoniae* Glc-DAG-s2 antigen presents unusual chemical features in both its lipidic and polar portions when compared to the previously characterized iNKT cell microbial antigens from *Sphingomonas* spp. or *Borrelia burgdorferi*. Instead of the α-galactose or α-galacturonic acid found on these antigens, and on the prototypical antigen α-GalCer, the otherwise weaker α-glucose is found in *S. pneumoniae* as well as in another gram-positive pathogen, GBS. Furthermore, the sugar is α-linked to a DAG backbone containing on position *sn*-2 the uncommon *cis*-vaccenic acid. Despite containing a glucose sugar, Glc-DAG-s2 was at least as active as the *Borrelia* BbGL-2c lipid in activating a mouse iNKT cell hybridoma and it showed similar antigenic potency in vivo (Figure 4B; [8]). Interestingly, we show here and in the previous studies that these unusual features are required together for the glycosylated DAG lipid to have any measurable antigenic potency. These stringent requirements were correlated with unusual binding kinetics compared to the *B. burgdorferi* DAG antigens, characterized by slow association and slow dissociation rates of the mCD1d-ligand complex to the iNKT TCR [8]. The structure of the mCD1d-Glc-DAG-s2-TCR complex presented here, together with the other studies we have carried out, allow us to understand the stringent chemical requirements, as well as the distinct TCR binding kinetics, in the recognition of the DAG antigens from these highly pathogenic bacteria.

As for the other DAG antigen, BbGL-2c, the iNKT TCR is able to induce conformational changes on both the Glc-DAG-s2 ligand and mCD1d (Figures 2 and 5A), which result in a conserved binding mode, as well as a weaker affinity, typical of the DAG antigens compared to their glycosphingolipid counterparts [14,22]. However, due to the presence of glucose, with a different conformation of its 4′ hydroxyl group compared to galactose, a hydrogen bond with the CDR1α of the TCR is lost, while a new contact with Gly155 on the α2 helix of CD1d is formed. While this alteration does not translate to an overall change in TCR affinity at equilibrium, it has profound effects on the kinetics of binding of the antigen complex with mCD1d by the iNKT cell TCR. Previous studies showed that contacts between the ligand and the TCR dominate the initial association phase, while protein-protein (and ligand-protein) contacts affect the stability of the complex [9]. Therefore, the loss of a contact with the α chain of the TCR can account for the slower TCR association rate exhibited by this ligand. Interestingly, the iNKT TCR appears to be especially sensitive to the conformation of the 4′-OH group, with glucose-containing antigens showing generally reduced potency (in terms of cytokine release by iNKT cells) [9,10] and preferential proliferation of Vβ7+ cells [10] compared to α-GalCer. Furthermore, the consequent locking of the glucose head in the favorable position following TCR engagement, described here for Glc-DAG-s2, likely contributes to a slower dissociation. These novel contacts rely on the presence of both the vaccenic acid and glucose, as the variants with an oleic acid in place of the vaccenic acid, or a galactose replacing the glucose, are considerably less active. Consistent with this, a model of Gal-DAG-s2 suggests that the presence of an axial 4′ hydroxyl would be located in an unfavorable position for recognition by the iNKT TCR (Figure S2). Moreover, the antigenicity of the ligand requires vaccenic acid to be in the *sn*-2 position of the ligand in order to orient correctly the glucose for recognition by the TCR. Interestingly, these structural requirements do not appear to be influenced by the variable CDR3β loop, as three different hybridomas responded to Glc-DAG-s2 at comparable levels (Figure 5C).

Glc-DAG-s2 also stimulates human iNKT cells [8] but is not clear whether the same stringent requirements observed in mouse are conserved in the human CD1d-TCR interaction as no structural information is available on the modality of recognition of DAG antigens by the human iNKT TCR. Clearly, more work has to be done to illuminate the structural basis of microbial DAG recognition by human iNKT cells.

Consistent with a model in which the TCR contacts first the ligand and subsequently CD1d, our mutational data also show that the protein-protein interface above the F′ pocket is critical for the interaction, and specifically, that this region determines the dissociation rate, and therefore the stability, of the mCD1d-TCR complex (Figure 6). Interestingly, the mechanism of antigen recognition by the iNKT TCR appears to be radically different to what has been observed for MHC-TCR interactions, where the TCR first contacts residues on the antigen presenting molecule and only a later stage contacts the antigen itself [23].

The extensive amount of structural and biochemical information recently collected on the interaction between CD1d and the iNKT TCR is consistent with the idea of the iNKT TCR as a pattern recognition receptor [10,12–14,18]. While the *S. pneumoniae* antigen follows the typical pattern of an α-linked sugar to a diacyl backbone, the data presented here show clearly that, within this pattern, stringent requirements are still in place. In particular, the Glc-DAG-s2 ligand exemplifies the case of a relatively weak hexose and an uncommon alkyl chain synergistically contributing to the potency of an iNKT antigen.

## Materials and Methods

### Protein Expression and Purification

The expression and purification methods of fully glycosylated mouse CD1d/β2m heterodimer proteins were reported previously [11]. Mouse TCR refolding was performed according to previously reported protocols [14] with minor modifications. 64 mg of α chain and 96 mg of β chain inclusion bodies were mixed together and added drop wise to 1 L refolding buffer (50 mM Tris-HCl, 0.4 M L-arginine, 5 M urea, 2 mM EDTA, 5 mM reduced glutathione, 0.5 mM oxidized glutathione, 0.2 mM PMSF, pH 8.0 at RT) two times. The refolding mix was dialyzed twice against 18 L dialysis buffer 1 (10 mM Tris-HCL, 0.1 M urea, pH 8.0) for 16 h and then once against 18 L of 10 mM Tris-HCl pH 8.0 for 24 h. The refolded TCR proteins were purified by MonoQ 5/50 GL (GE Healthcare) using a linear NaCl gradient (0–300 mM NaCl) followed by size exclusion chromatography using a Superdex S200 10/300 GL (GE Healthcare) in 50 mM Hepes pH 7.5, 150 mM NaCl.

### Glycolipid Loading and Ternary Complex Formation

The synthetic DAG ligand Glc-DAG-s2 was synthesized as previously reported [8] and dissolved at 4 mg/ml in DMSO. mCD1d was incubated overnight with 3–6 molar excess of Glc-DAG-s2 in presence of 0.05% Tween-20 and 100 mM Tris-Cl pH 7.0. Glc-DAG-s2 loaded CD1d was purified by size exclusion chromatography first and then incubated with equimolar amount of TCR for 30 min without further purification. The complex was concentrated to 4.8 mg/ml for crystallization.

### Crystallization and Structure Determination

Crystals of mCD1d-Glc-DAG-s2-TCR complexes were grown at 22.3°C by sitting drop vapor diffusion while mixing 0.5 µl protein with 0.5 µl precipitate (17% polyethylene glycol 3350, 8% v/v Tacsimate pH 5.0). Crystals were flash-cooled at 100 K in mother liquor containing 20% glycerol. Diffraction data were collected at the Stanford Synchrotron Radiation Laboratory (SSRL) beamline 7.1 and processed with the iMosflm software [24]. The mCD1d-Glc-DAG-s2-TCR crystal belongs to space group $C222_1$ with cell parameters $a = 78.1$ Å; $b = 190.7$ Å; $c = 150.9$ Å. The asymmetric unit contains one mCD1d-glycolipid-TCR molecule with an estimated solvent content of 55.0%. The structures were determined by molecular replacement using MOLREP as part of the CCP4 suite [25,26] using the protein coordinates from the mCD1d-iGb3 structure (PDB code 2Q7Y) [27], followed by the Vα14Vβ8.2 TCR [14] (from PDB code 3O8X) as the search model. When a MR solution containing both mCD1d and TCR was obtained, the model was rebuilt into $\sigma_A$-weighted $2F_o–F_c$ and $F_o–F_c$ difference electron density maps using the program COOT [28]. Maximum-likelihood restrained refinement coupled with TLS refinement was performed in REFMAC [29] with five anisotropic domains (α1-α2 domain of CD1d, including carbohydrates and glycolipid, α3-domain, β2m, variable domains and constant domains of the TCR). The quality of the model was evaluated with the program Molprobity [30] and the validation tools available in COOT. Shake-omit maps were generated by removing the ligand from the structure and randomly perturbating the coordinates, occupancy, and B-factor of each atom by 0.2 Å, 0.05 units, and 20 $Å^2$, respectively, with the software Moleman2 [31]. The resulting structure was then refined with the software REFMAC as described earlier. Data collection and refinement statistics are presented in Table 1. Coordinates and structure factors have been deposited in the Protein Data Bank under accession code 3TA3.